Implications of Redshift Space Distortions

Cosmological Quests for the Next Decades
April 20th 2017

Yong-Seon Song
(Korea Astronomy and Space Science Institute)


Cris Sabiu


Yi Zheng


Minji Oh

CosKASI
Cosmology Group at
Korea Astronomy and Space Science Institute

CosKASI

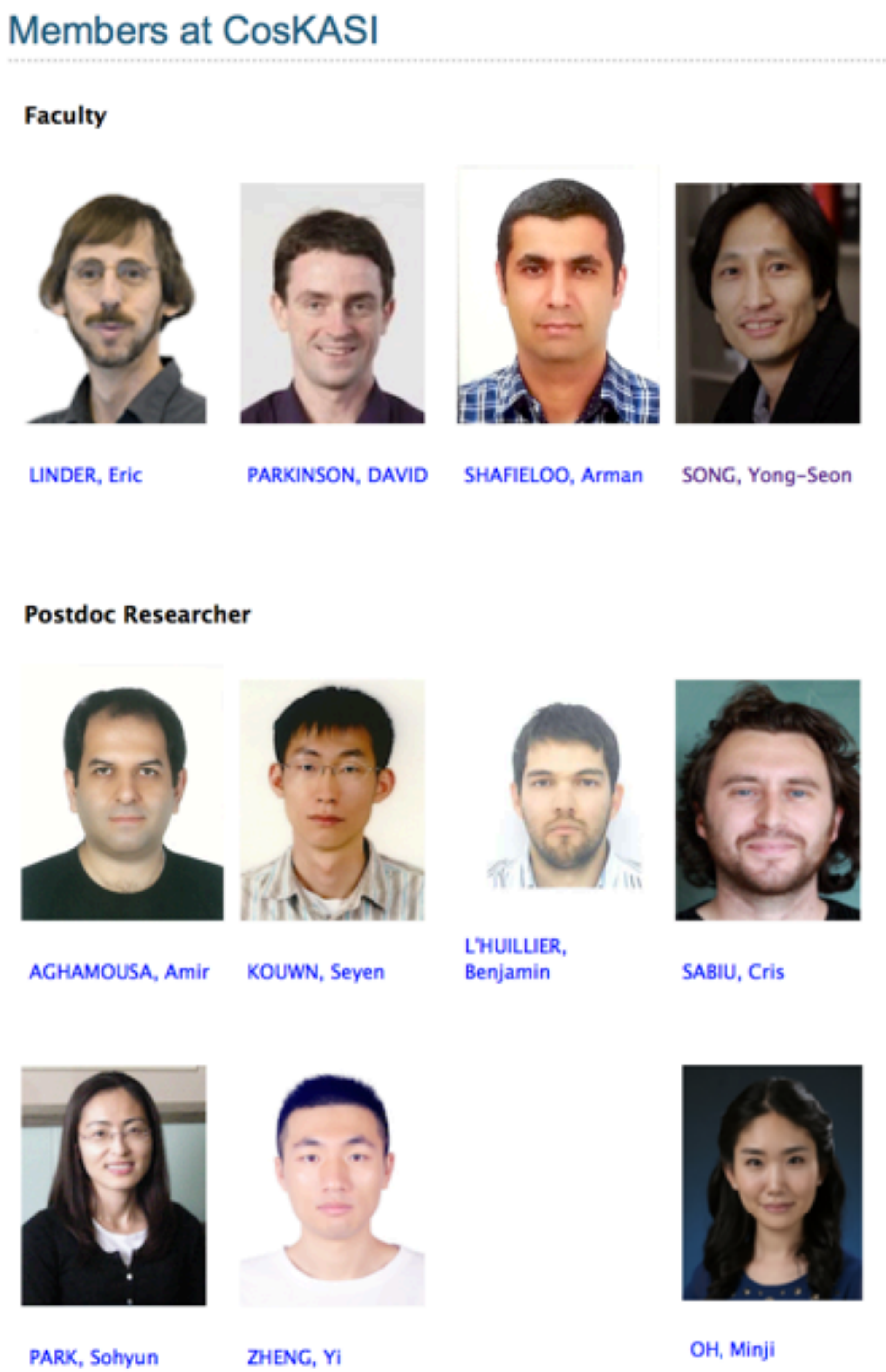

Initiated in 2014

Group is selected as BIG ISSUE GROUP in 2016

Participate in DESI and LSST

Survey Science End-to-End

Survey → Simulation

→ Analysis (new estimator & perturbation theory

→ Theoretical models

→ Standard model or Surprising

Cris Sabiu

Yi Zheng

Minji Oh

Physical Cosmology.

Arman Shafieloo

-Reconstructing dark energy/
Falsifying Lambda

-Reconstructing primordial spectrum/
Falsifying power-law

-Testing isotropy/homogeneity/metric/
curvature

-Playing with toys (inflation model building, dark energy model building, surviving some non-local gravity models, finding systematics, criticizing others, etc) .

Dr. Amir Aghamousa
Start Date: 01/05/2016

-Strong lens systems time delay estimation

-Supernova light curve analysis

-Non-parametric estimation of the CMB angular power spectrum/testing standard model (REACT, GP)

-Advance statistics

Dr. Benjamin L'Huillier
Start Date: 01/03/2016

-Model independent test of metric/
curvature/isotropy

-Distinguishing early universe scenarios using large scale structure data/N-body simulations

-Supernovae light curve analysis

-N-body simulations to test gravity.

Research Outline

- Large area cosmological redshift surveys
  - Cross correlations between massive (galaxies) and massless particles (photons)
  - Tests of shielding mechanisms
  - Fifth-forces - stochastic velocity bias
- Cosmology with large area radio surveys (EMU)
  - P(k) beyond the turnover: relativistic effects, extra-species, non-Gaussianity
- Machine learning in cosmology
  - Object classification (SN spectra, radio galaxy cross-ID)
  - Unsupervised learning - ‘unknown unknowns’

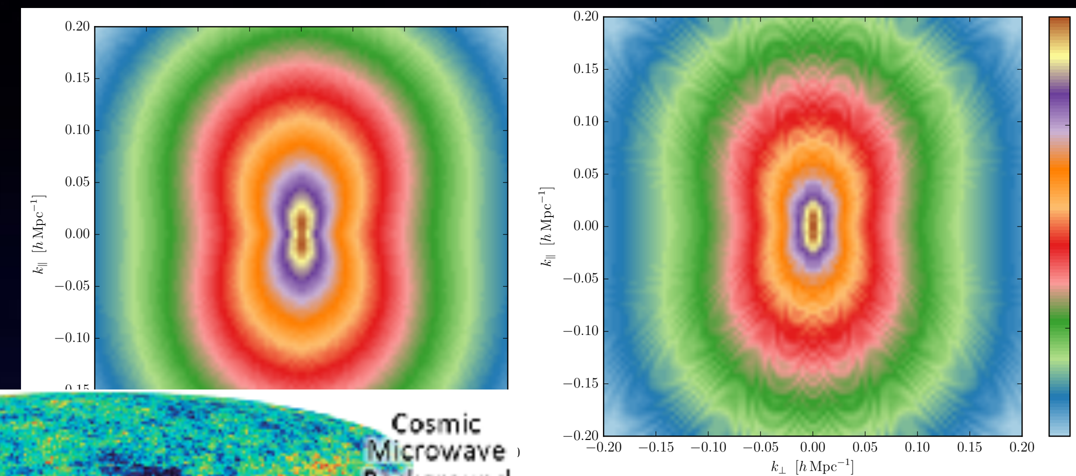

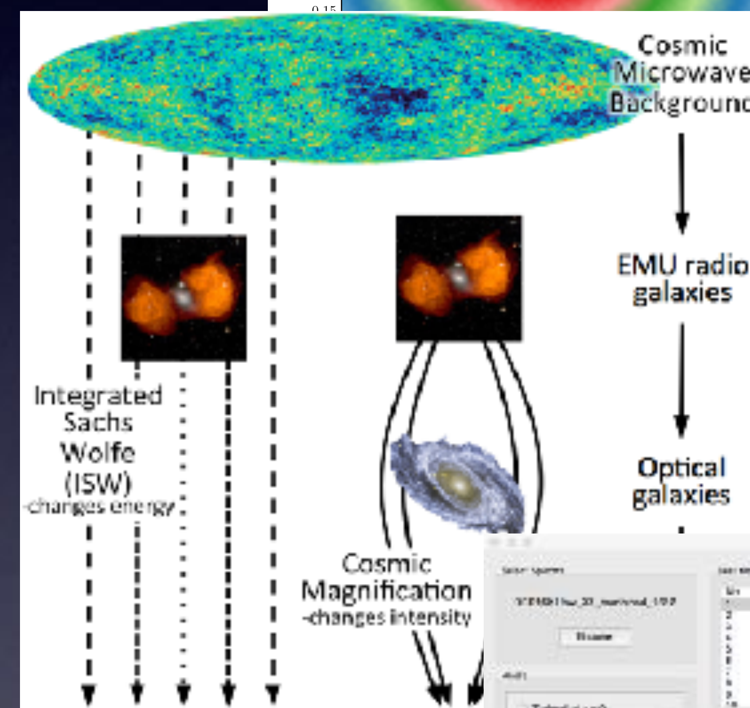

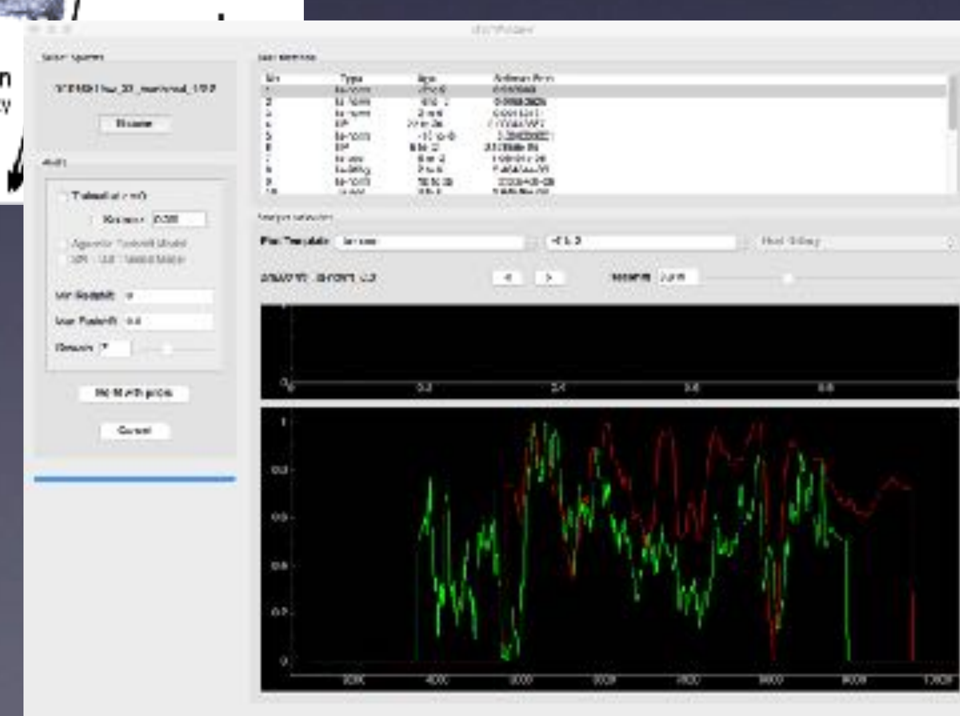

Galaxy clustering seen in redshift space

- Spectroscopy wide surveys have provided the key observables of distance measures and growth functions, such as 2dF, SDSS, WiggleZ, BOSS

- Most unknowns in the universe will be revealed through LSS

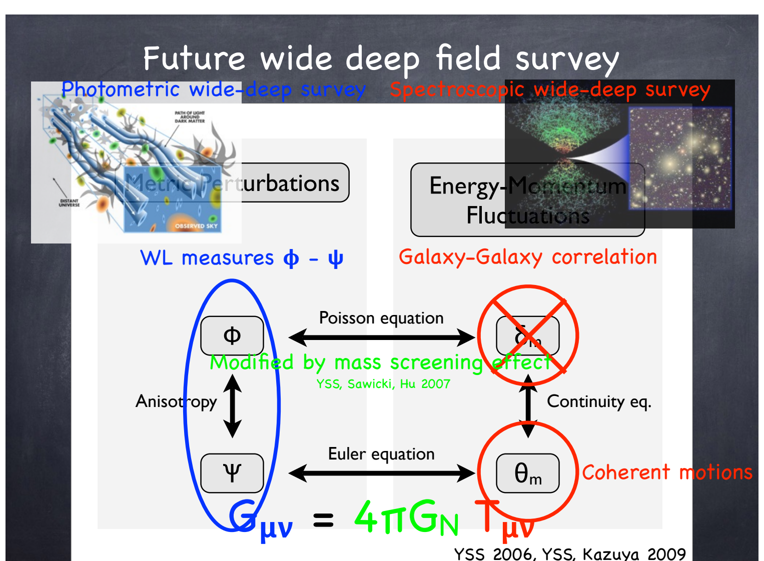

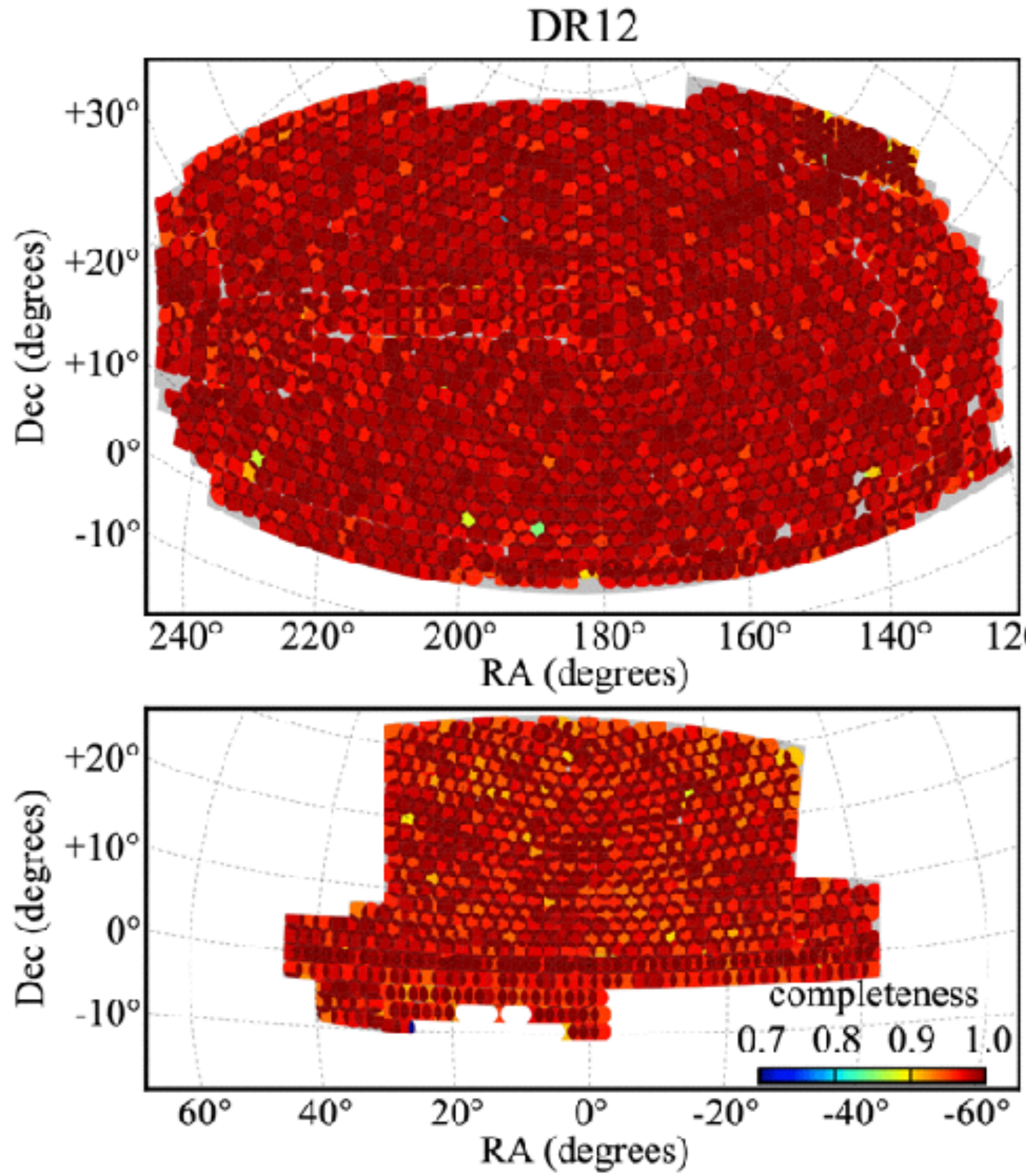

Alam et.al 2015; YSS, Koyama 2009

Standard ruler

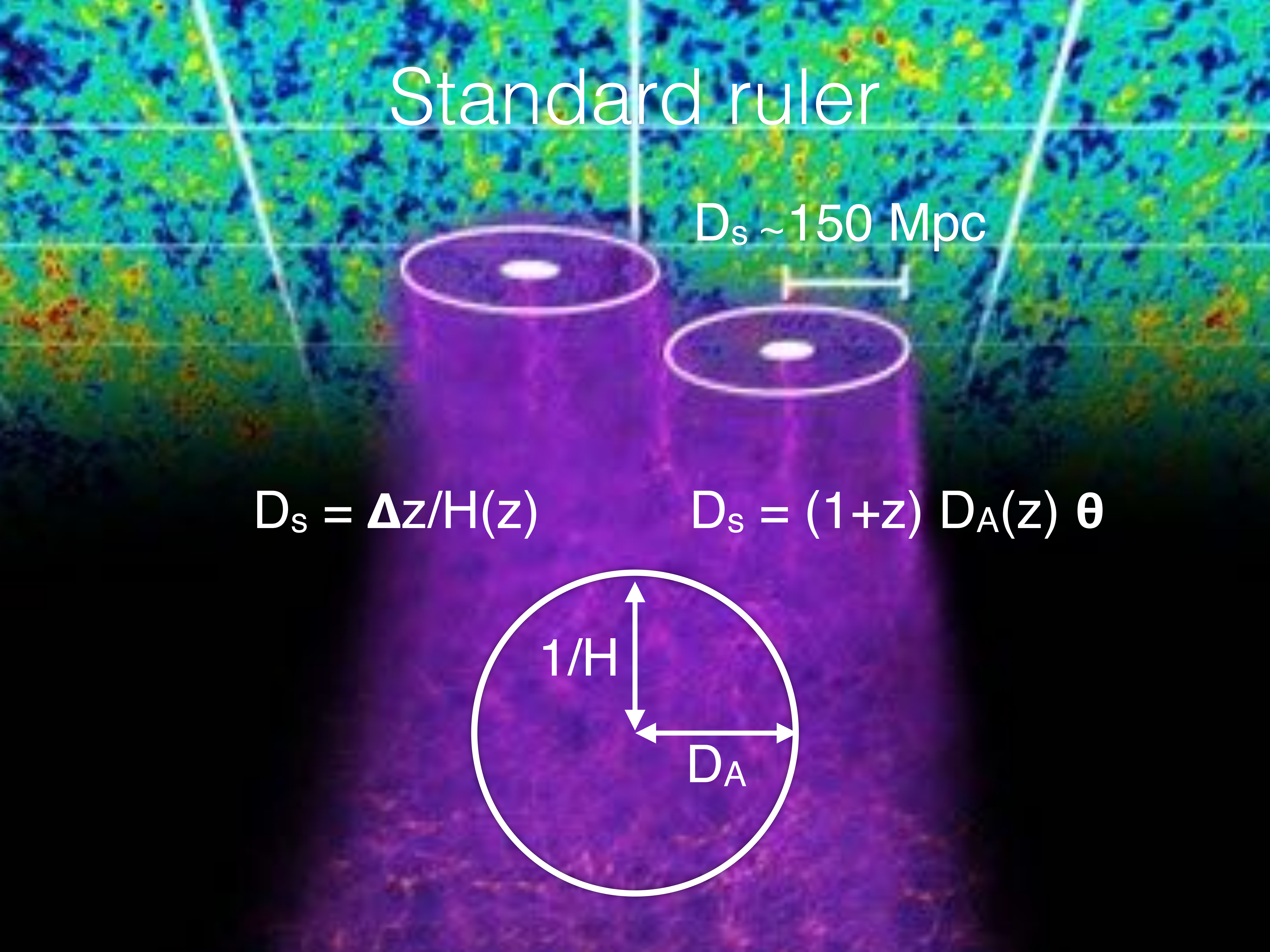

$D_S = \mathbf{\Delta} z/H(z)$ $\qquad$ $D_S = (1+z)\, D_A(z)\, \boldsymbol{\theta}$

Risk free option to determine cosmic distance

(D_A, H^{-1})

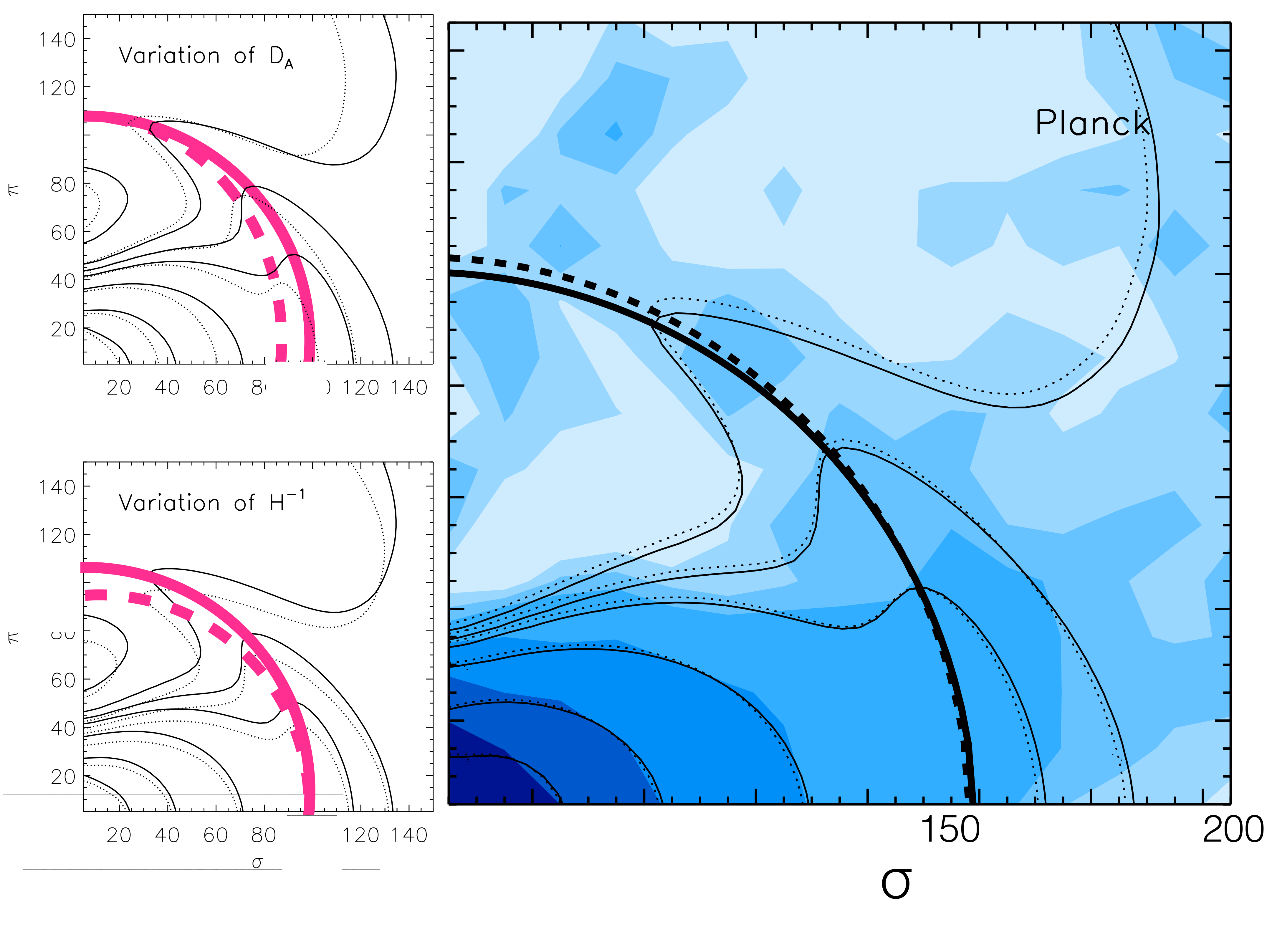

History and plan for spectroscopy surveys

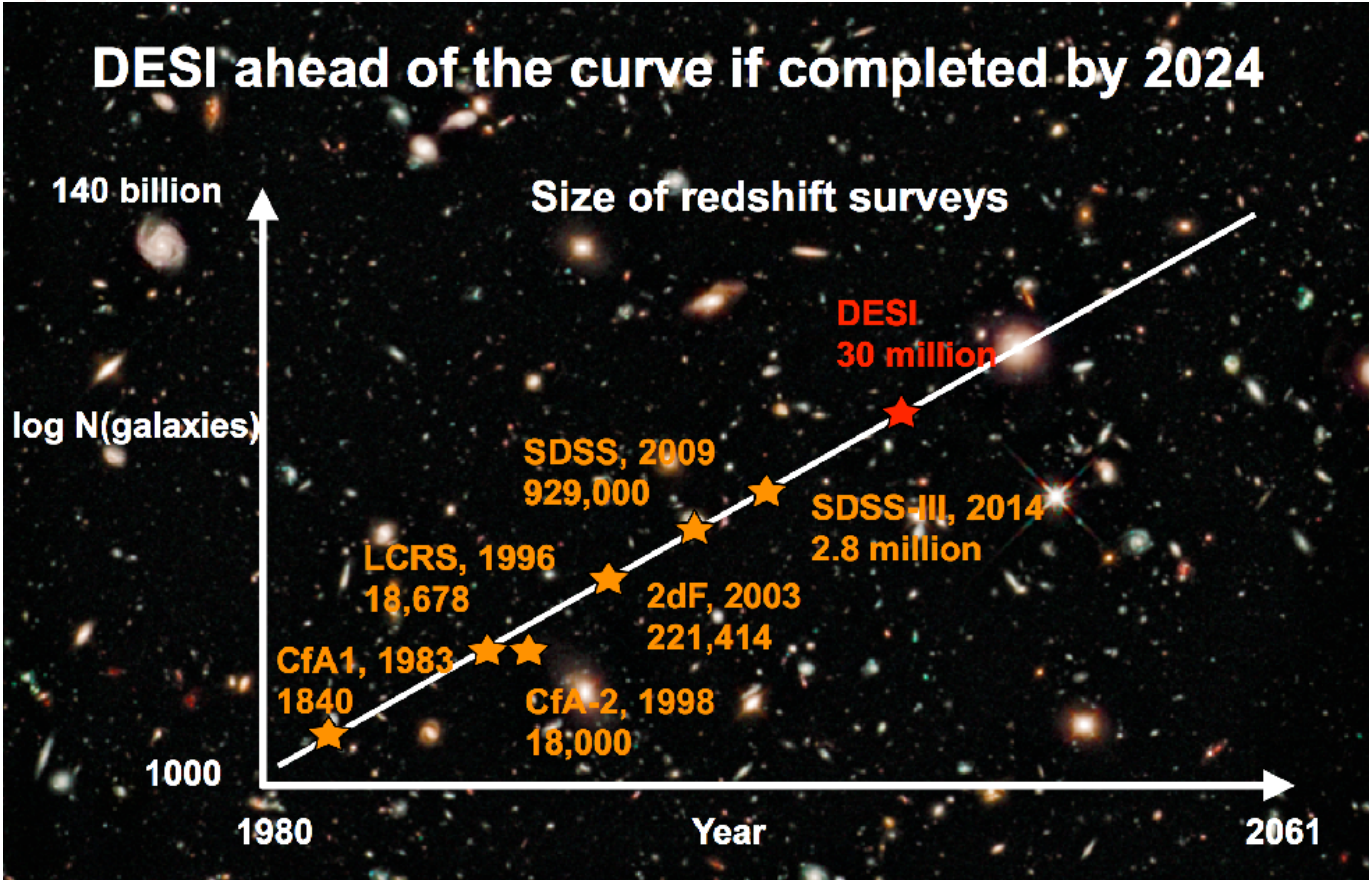

Implication of cosmic acceleration

- Breaking down our knowledge of particle physics: we have limited knowledge of particle physics bounded by testable high energy, and our efforts to explain the cosmic acceleration turn out in vain:

  Alternative mechanism to generate fine tuned vacuum energy

  New unknown energy component

  Unification or coupling between dark sectors

- Breaking down our knowledge of gravitational physics: gravitational physics has been tested in solar system scales, and it is yet confirmed at horizon size:

  Presence of extra dimension

  Non-linear interaction to Einstein equation

- Failure of standard cosmology model: our understanding of the universe is still standing on assumption:

  Inhomogeneous models: LTB, back reaction

Implication of cosmic acceleration

- Breaking down our knowledge of particle physics: we have limited knowledge of particle physics bounded by testable high energy, and our efforts to explain the cosmic acceleration turn out in vain:

Dynamical Dark Energy: modifying matter

Alternative mechanism to generate fine tuned vacuum energy

New unknown energy component

$$G_{\mu\nu} = 4\pi G_N T_{\mu\nu} + \Delta T_{\mu\nu}$$

Unification or coupling between dark sectors

- Breaking down our knowledge of gravitational physics: gravitational physics has been tested in solar system scales, and it is yet confirmed at horizon size:

Geometrical Dark Energy: modifying gravity

Presence of extra dimension

Non-linear interaction to Einstein equation

$$G_{\mu\nu} + \Delta G_{\mu\nu} = 4\pi G_N T_{\mu\nu}$$

- Failure of standard cosmology model: our understanding of the universe is still standing on assumption:

Inhomogeneous models: LTB, back reaction

Two windows on acceleration and gravitation

Their simultaneous determination allows for a consistency test and provides sensitivity to physics beyond the standard dark energy paradigm

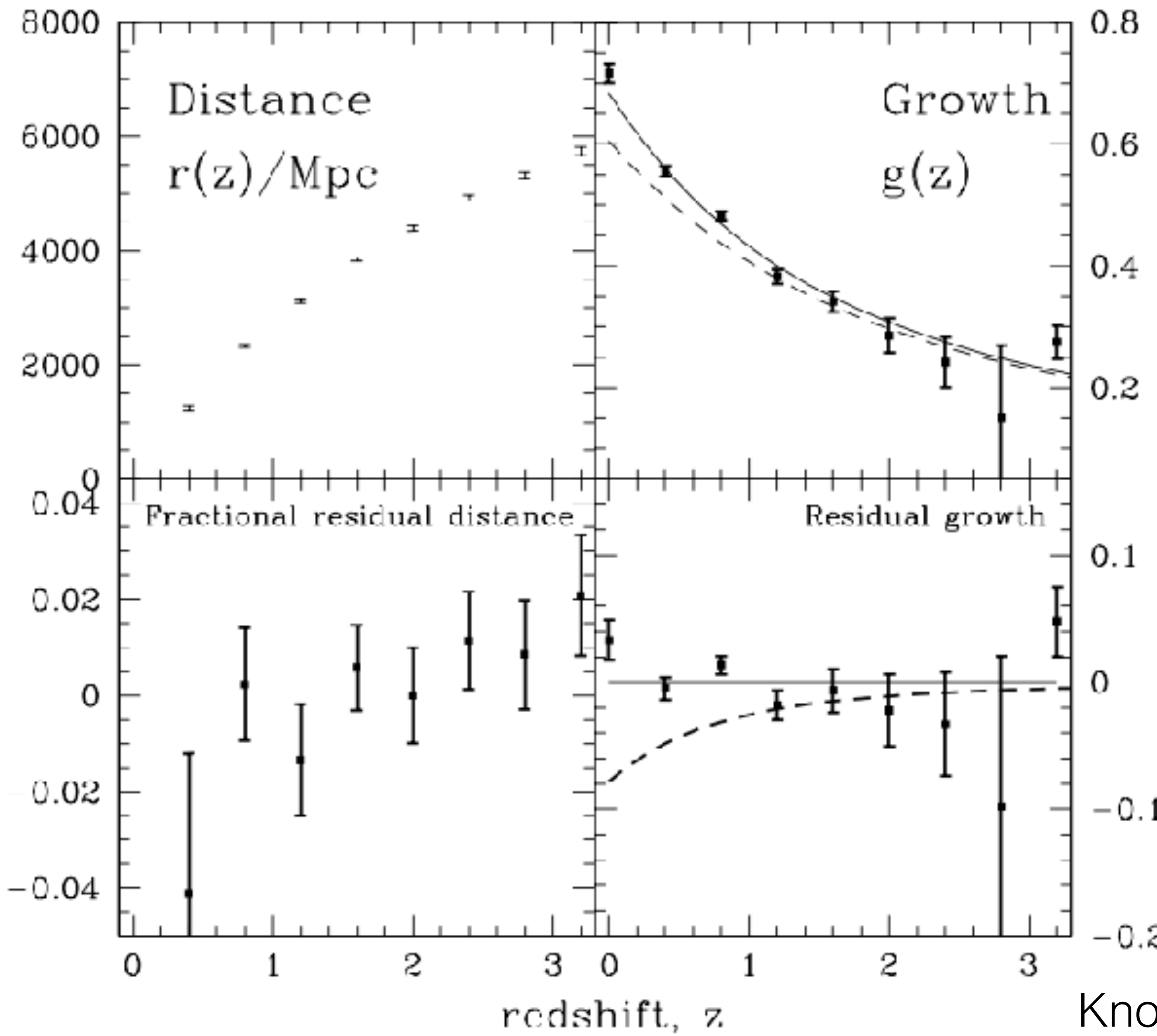

Knox, YSS, Tyson 2005

Galaxy clustering seen in redshift space

- Spe
  hav
  obs
  me
  fun
  Wig
- Mo
  will

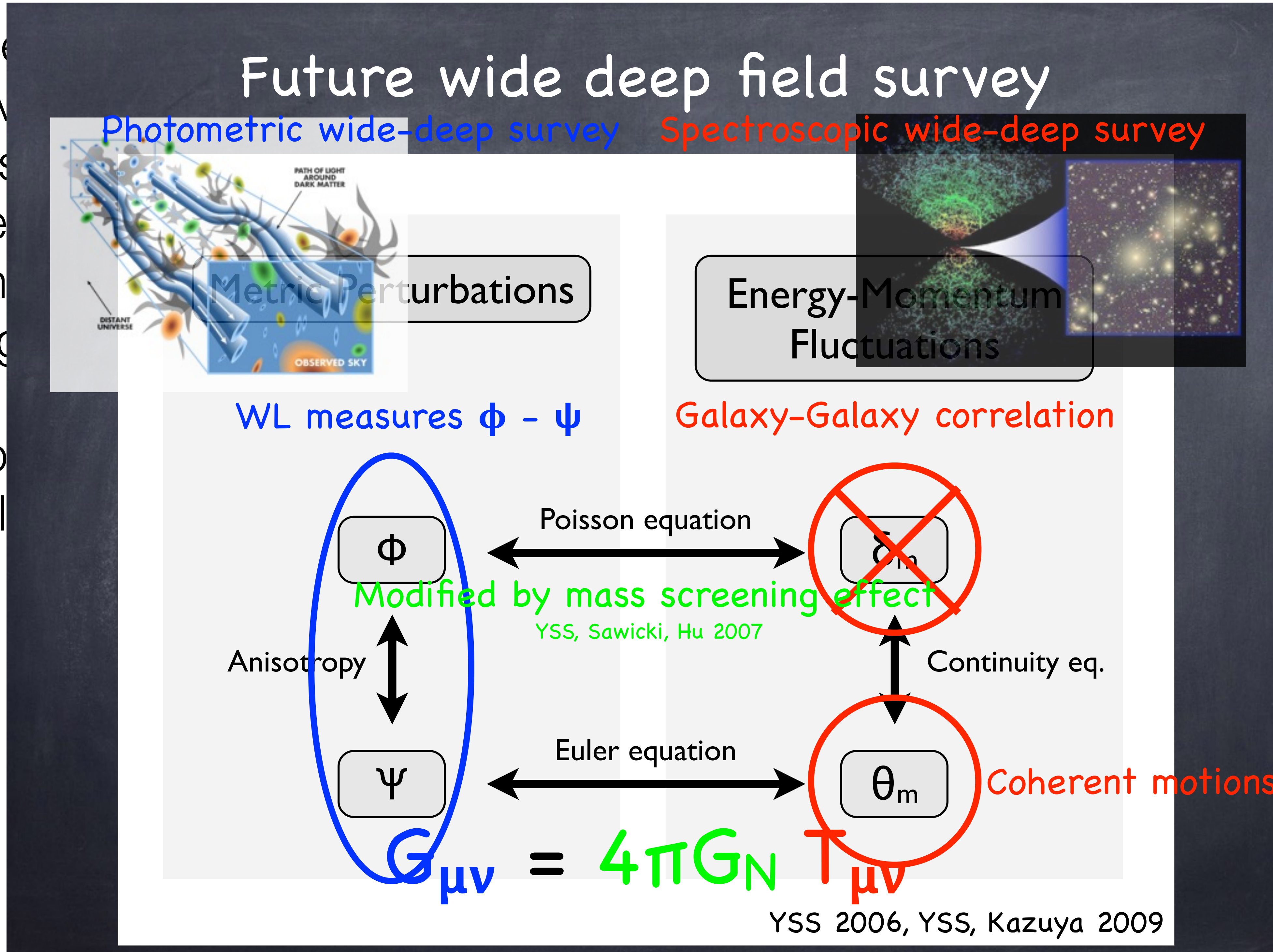

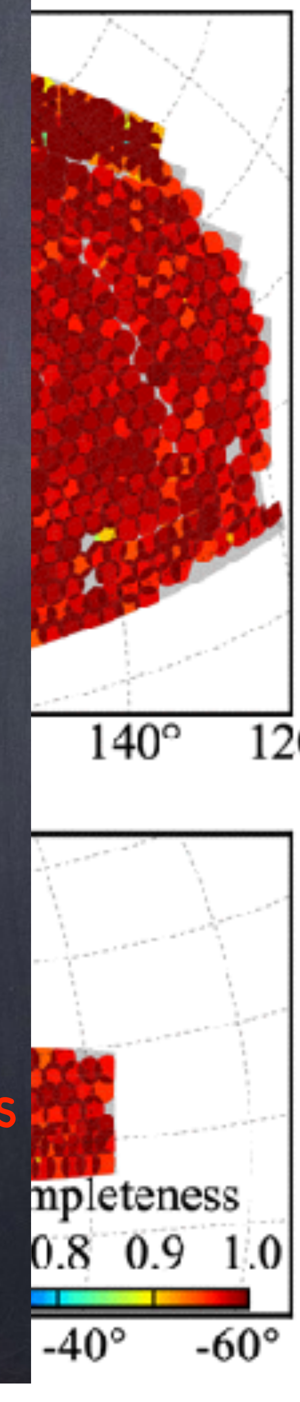

Cosmological probe of coherent motion

The first measured $f\sigma_8$

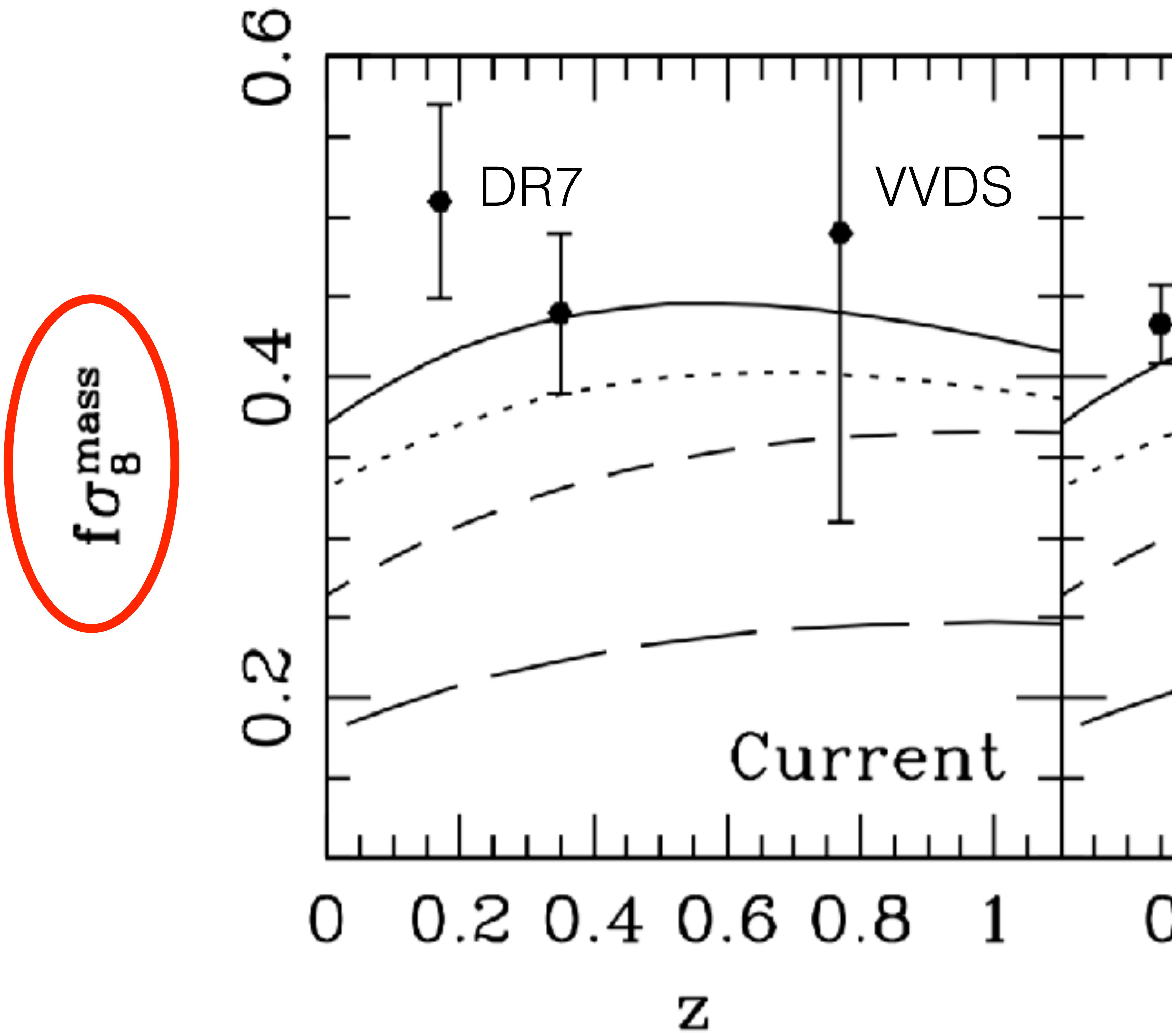

YSS, Percival 2009

Cosmological probe of coherent motion

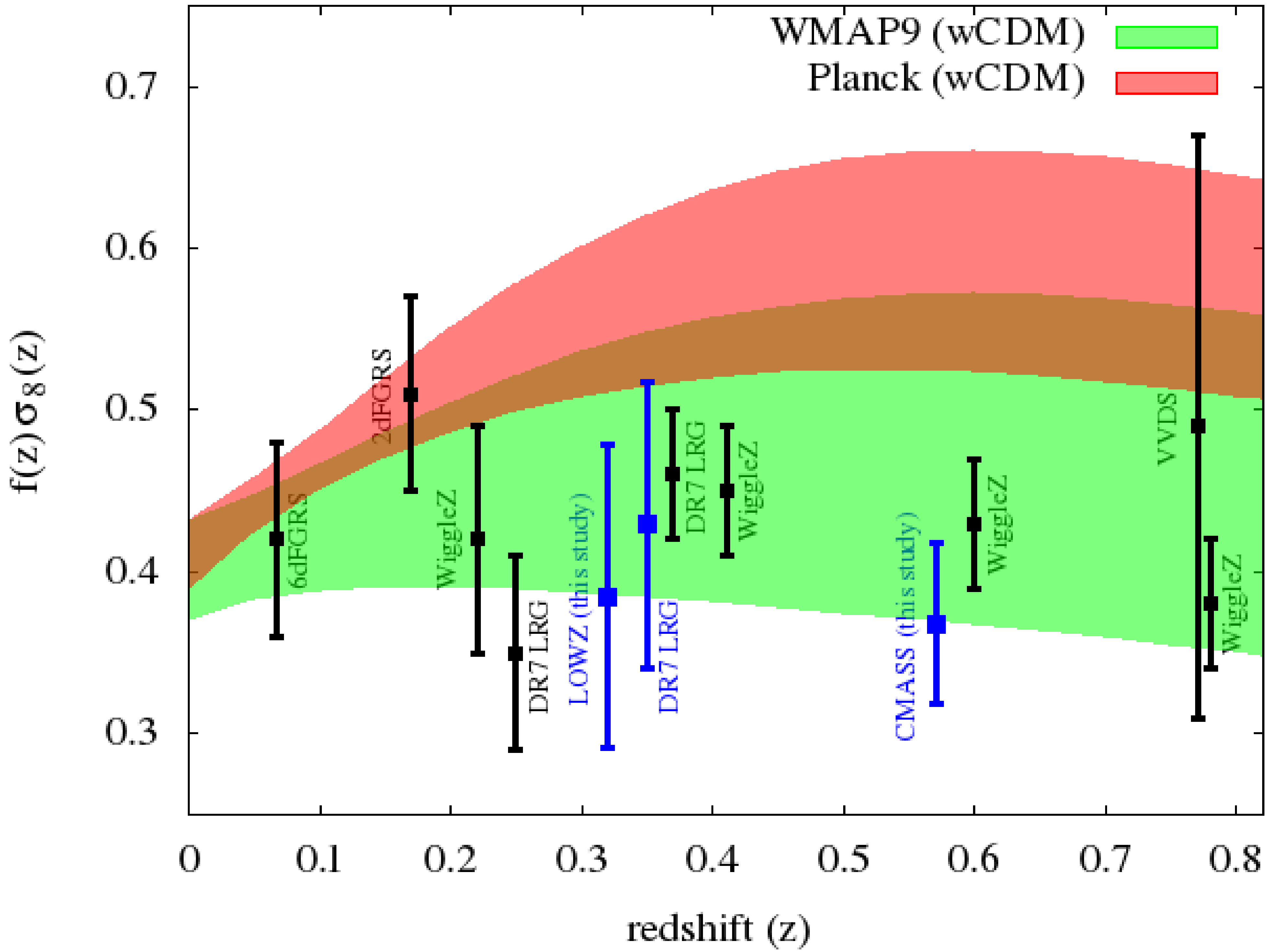

Cosmological probe of coherent motion

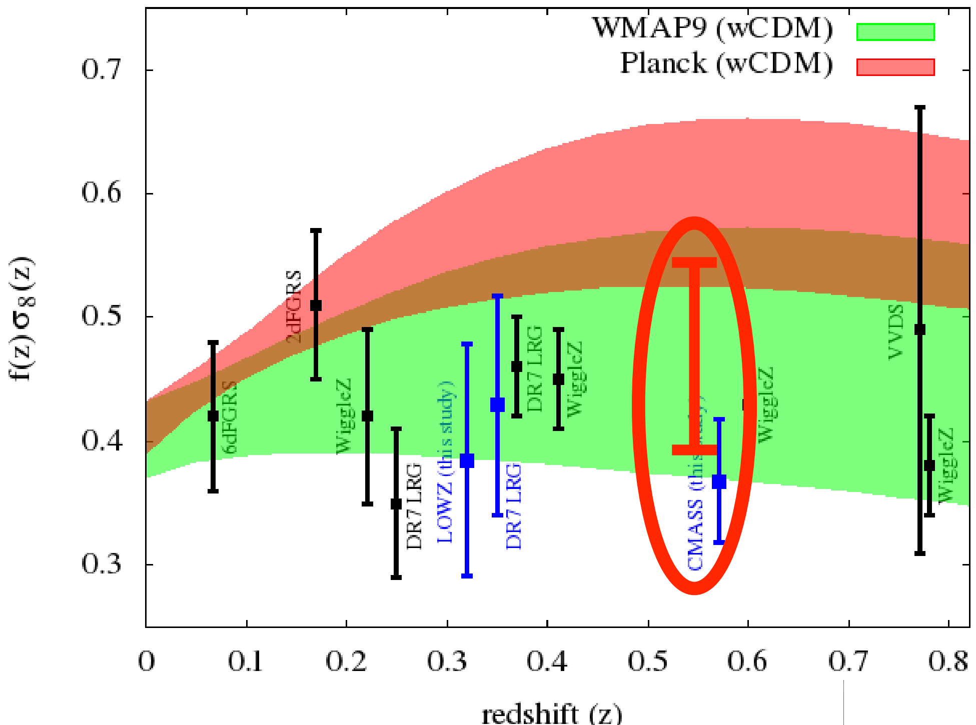

CMASS (Chuan et.al. 2015)

CMASS (YSS et.al. 2015)

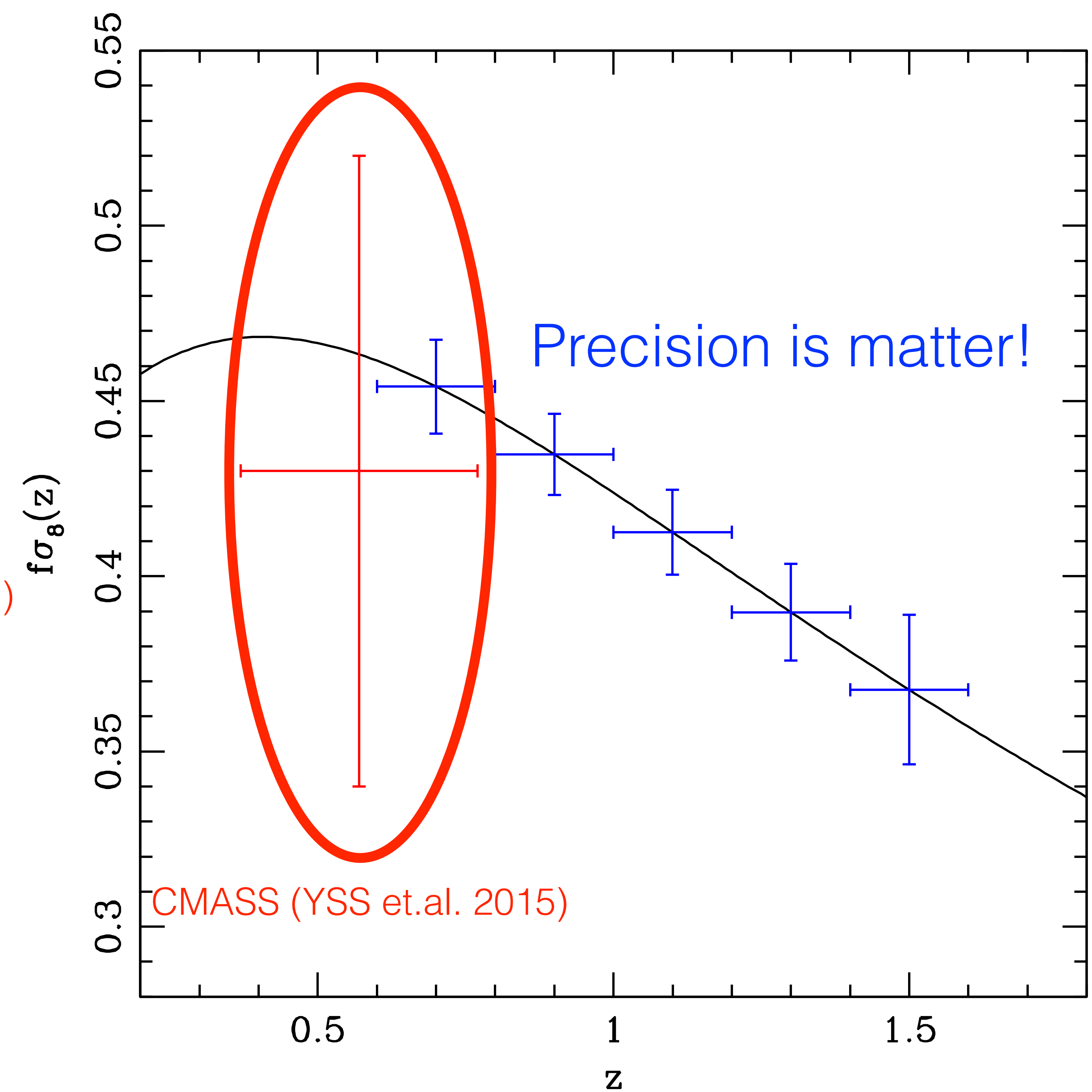

YSS, Taruya, Akira 2015

Power spectrum in redshift space

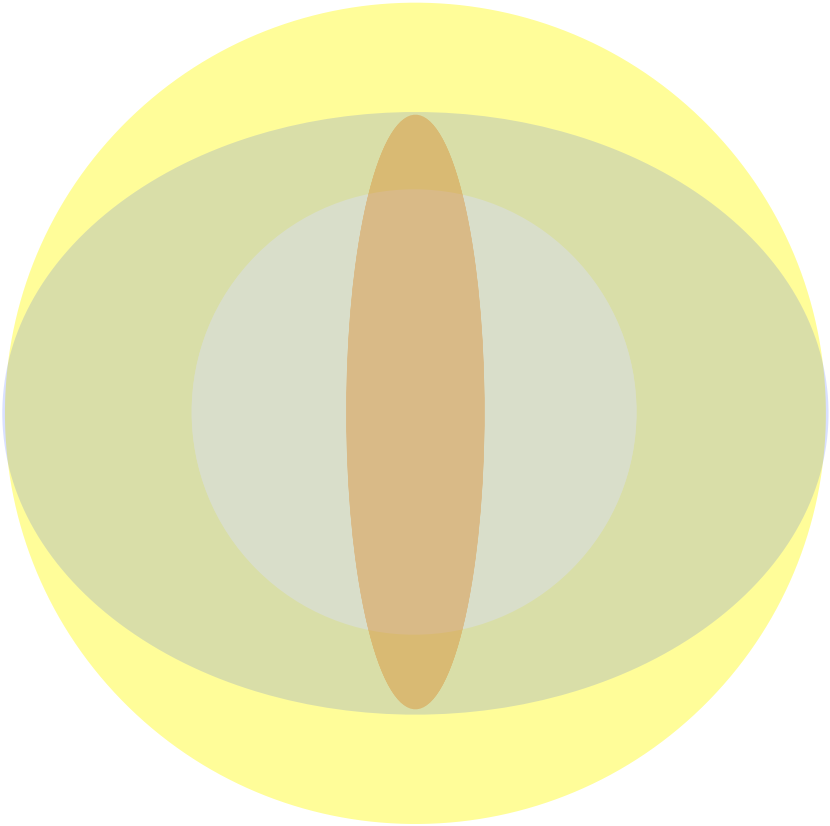

Squeezing effect at large scales

(Kaiser 1987)

$$P_s(k,\boldsymbol{\mu}) = P_{gg}(k) + 2\boldsymbol{\mu}^2 P_{g\boldsymbol{\theta}}(k) + \boldsymbol{\mu}^4 P_{\boldsymbol{\theta\theta}}(k)$$

Anisotropy correlation without corrections

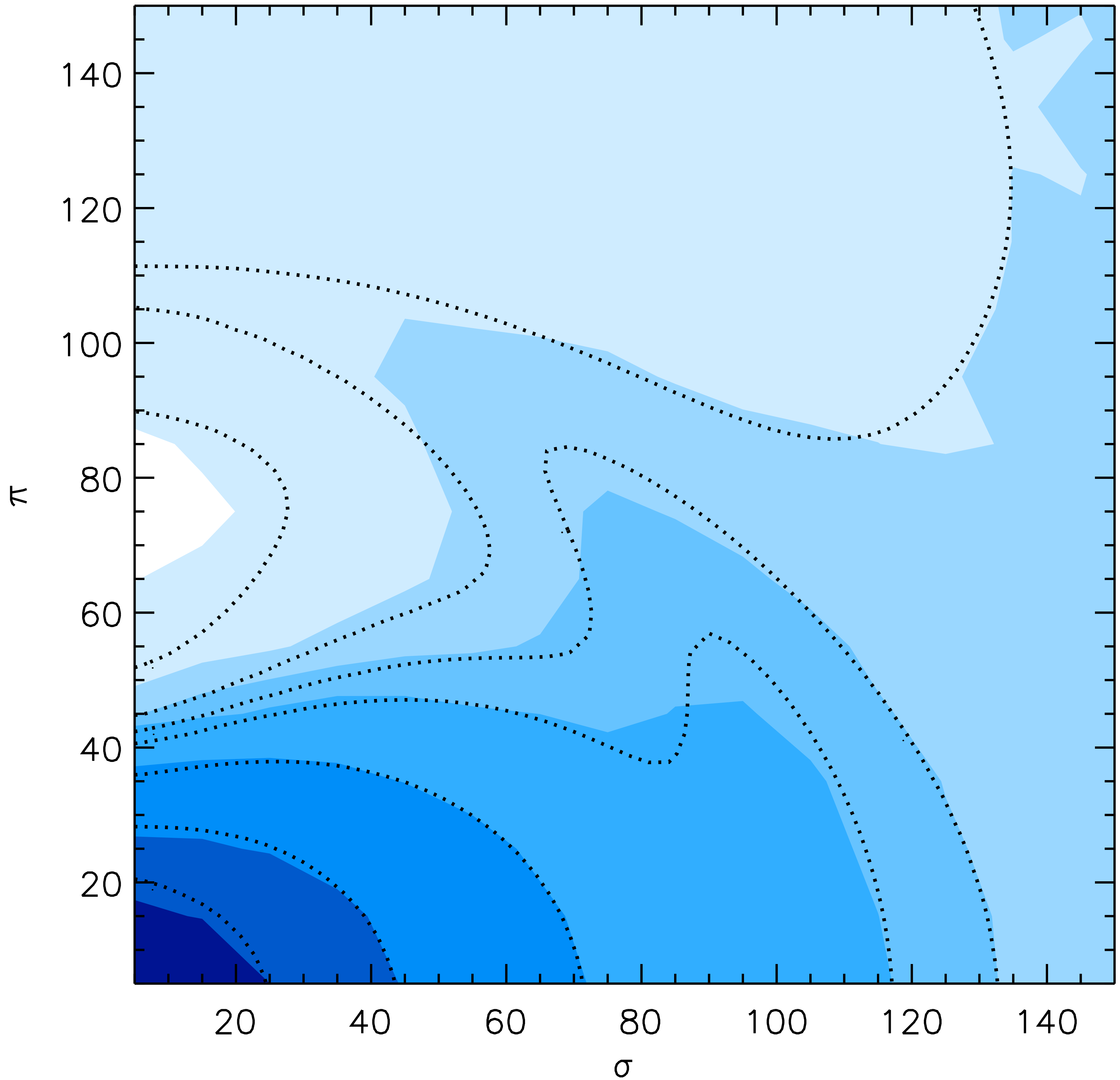

Power spectrum in redshift space

Squeezing effect at large scales

(Kaiser 1987)

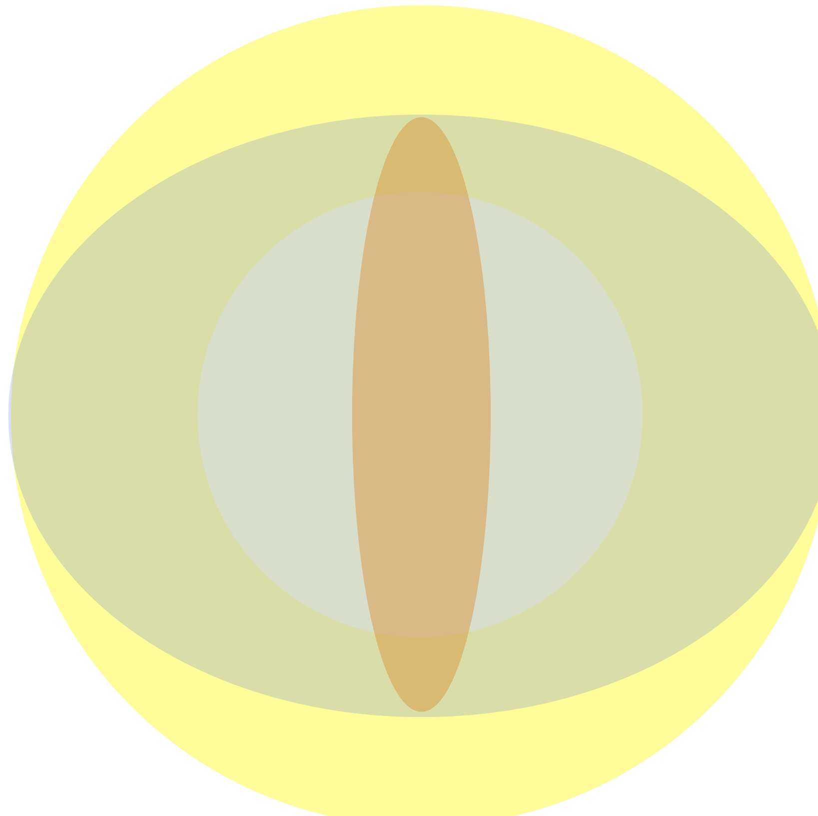

Non-linear corrections

Higher order polynomials

Finger of God effect

$$P_s(k,\boldsymbol{\mu}) = P_{gg}(k) + 2\boldsymbol{\mu}^2 P_{g\boldsymbol{\theta}}(k) + \boldsymbol{\mu}^4 P_{\boldsymbol{\theta\theta}}(k)$$

$$\downarrow$$

$$P_s(k,\mu) = [P_{gg}(k) + \Delta P_{gg} + 2\boldsymbol{\mu}^2 P_{g\Theta}(k) + \Delta P_{g\boldsymbol{\theta}} + \boldsymbol{\mu}^4 P_{\boldsymbol{\theta\theta}}(k) + \Delta P_{\boldsymbol{\theta\theta}}$$
$$+ \boldsymbol{\mu}^2 A(k) + \boldsymbol{\mu}^4 B(k) + \boldsymbol{\mu}^6 C(k) + \ldots]\ \exp[-(k\boldsymbol{\mu}\sigma_p)^2]$$

Taruya, Nishimichi, Saito 2010; Taruya, Hiramatsu 2008; Taruya, Bernardeau, Nishimichi 2012

Improved RSD model

$$P_s(k,\mu) = [Q_0(k) + \mu^2 Q_2(k) + \mu^4 Q_4(k) + \mu^6 Q_6(k)] \exp[-(k\mu\sigma_p)^2]$$

$$\xi(\sigma,\pi) = \int d^3k\ P(k,\mu) e^{ikx} = \Sigma \xi_l(s)\ \mathcal{P}_l(\nu)$$

$$\xi_\ell(s) = i^l \int k^2 dk\ P_l(k)\ j_l(ks)$$

$$P_0(k) = p_0(k)$$

$$P_2(k) = 5/2\ [3p_1(k) - p_0(k)]$$

$$P_4(k) = 9/8\ [35p_2(k) - 30p_1(k) + 3p_0(k)\ ]$$

$$P_6(k) = 13/16\ [231p_3(k) - 315p_2(k) - 105p_1(k) + 5p_0(k)\ ]$$

$$p_n(k) = 1/2\ [\ \gamma(n+1/2,\kappa)/\kappa^{n+1/2} Q_0(k) + \gamma(n+3/2,\kappa)/\kappa^{n+3/2} Q_2(k)$$

$$+ \gamma(n+5/2,\kappa)/\kappa^{n+5/2} Q_4(k) + \gamma(n+7/2,\kappa)/\kappa^{n+7/2} Q_6(k)$$

$$\kappa = k^2 \sigma^2_p$$

YSS, Okumura, Taruya 2014   Taruya, Nichimishi, Saito 2010

Anisotropy correlation without corrections

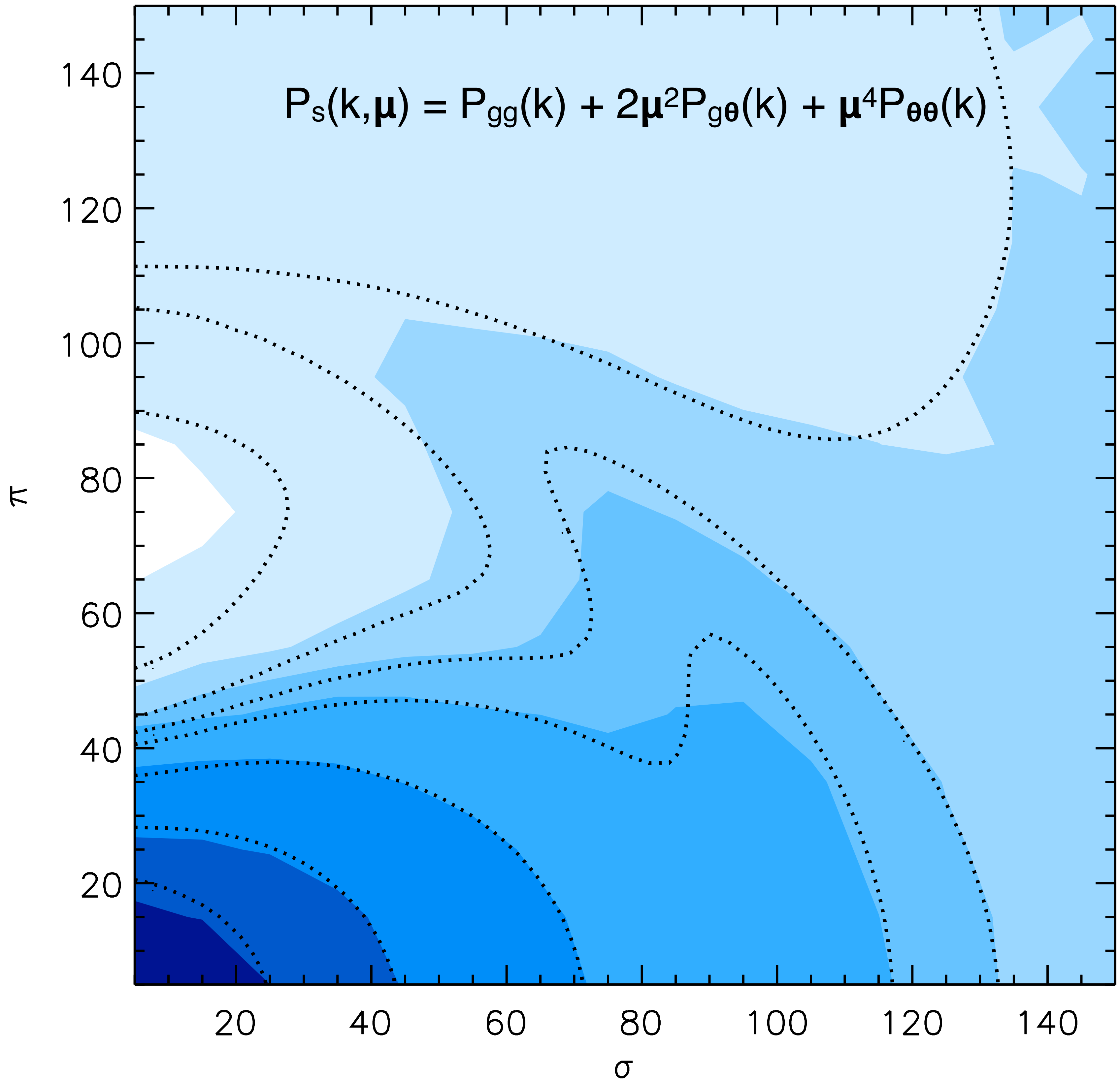

YSS et.al. 2015

Anisotropy correlation with corrections

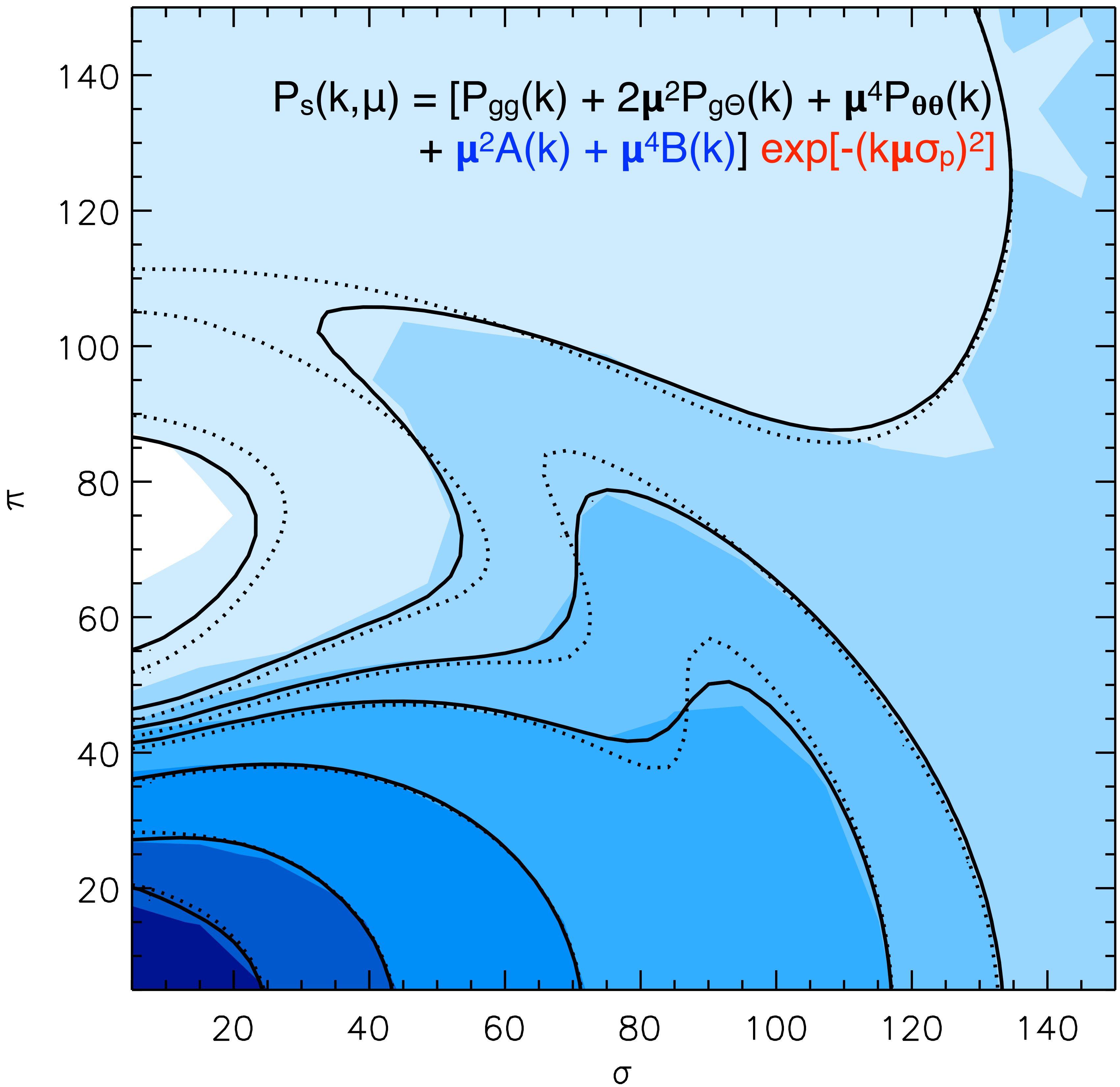

YSS et.al. 2015

Mapping of clustering from real to redshift spaces

$$P_s(k,\boldsymbol{\mu}) = \int d^3x\, e^{ikx} \langle \boldsymbol{\delta\delta} \rangle$$

$$\Downarrow$$

$$P_s(k,\mu) = \int d^3x\, e^{ikx} \langle e^{jv} (\boldsymbol{\delta}+\boldsymbol{\mu}^2\Theta)(\boldsymbol{\delta}+\boldsymbol{\mu}^2\Theta)\rangle$$

$$= \int d^3x\, e^{ikx} \exp\{\langle e^{jv}\rangle_c\} \left[\langle e^{jv}(\boldsymbol{\delta}+\boldsymbol{\mu}^2\Theta)(\boldsymbol{\delta}+\boldsymbol{\mu}^2\Theta)\rangle_c + \langle e^{jv}(\boldsymbol{\delta}+\boldsymbol{\mu}^2\Theta)\rangle_c \langle e^{jv}(\boldsymbol{\delta}+\boldsymbol{\mu}^2\Theta)\rangle_c\right]$$

- Non-linear corrections: there is limit in the perturbative approach at smaller scales. We need find a way to combine the simulation result.
- Higher order polynomials: there is an infinite tower of cross correlation between velocity and density fields. We have to decide the order limit.
- The FoG effect: the exact functional form is unknown. Only thing that we know is that it is a function of velocity dispersion σ_p.

Mapping of clustering from real to redshift spaces

$$P_s(k,\boldsymbol{\mu}) = \int d^3x\, e^{ikx} \langle \boldsymbol{\delta\delta} \rangle$$

$$\Downarrow$$

$$P_s(k,\mu) = \int d^3x\, e^{ikx} \langle e^{jv} (\boldsymbol{\delta}+\boldsymbol{\mu}^2\Theta)(\boldsymbol{\delta}+\boldsymbol{\mu}^2\Theta)\rangle$$

$$= \int d^3x\, e^{ikx} \exp\{\langle e^{jv}\rangle_c\} [\langle e^{jv}(\boldsymbol{\delta}+\boldsymbol{\mu}^2\Theta)(\boldsymbol{\delta}+\boldsymbol{\mu}^2\Theta)\rangle_c + \langle e^{jv}(\boldsymbol{\delta}+\boldsymbol{\mu}^2\Theta)\rangle_c \langle e^{jv}(\boldsymbol{\delta}+\boldsymbol{\mu}^2\Theta)\rangle_c]$$

$$P_s(k,\mu) = [P_{gg}(k) + 2\boldsymbol{\mu}^2 P_{g\Theta}(k) + \boldsymbol{\mu}^4 P_{\boldsymbol{\theta\theta}}(k) + A(k,\boldsymbol{\mu}) + B(k,\boldsymbol{\mu}) + T(k,\boldsymbol{\mu}) + F(k,\boldsymbol{\mu})]$$

$$\exp[-(k\boldsymbol{\mu}\sigma_p)^2]$$

See Yi's Talk on Thu

- Higher order polynomials are generated by density and velocity cross-correlation which generate the infinite tower of correlation pairs. We take the perturbative approach to cut off higher orders.
- The FoG effect consists of the one-point contribution and the correlated velocity pair contribution. The latter is perturbatively expanded as F term, and the former is parameterised using σ_p.

Yi, YSS 2016

Precision & Accuracy

The conservative measurement of growth function with k_{max}<0.1h/Mpc

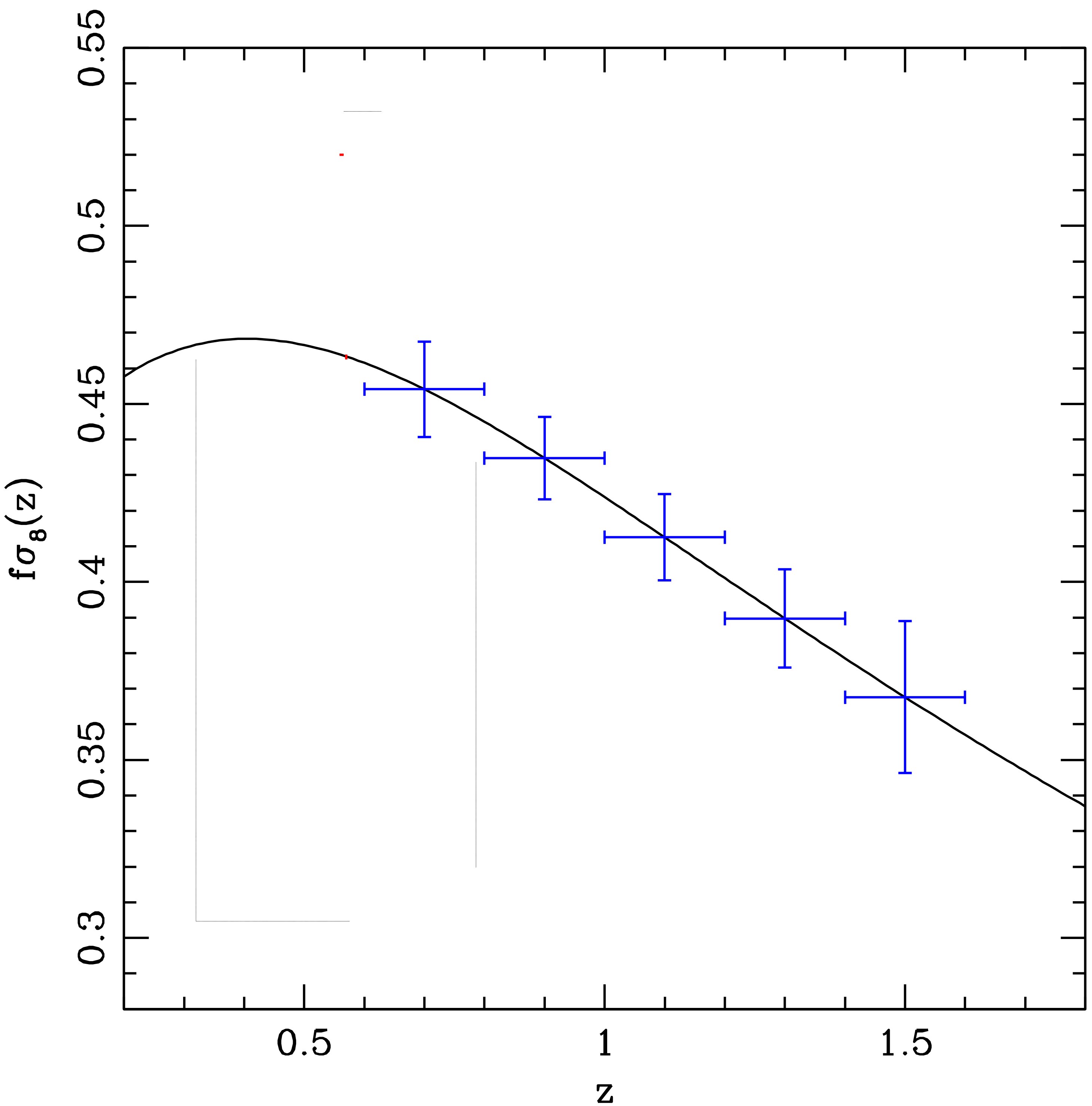

Galaxy clustering seen in redshift space

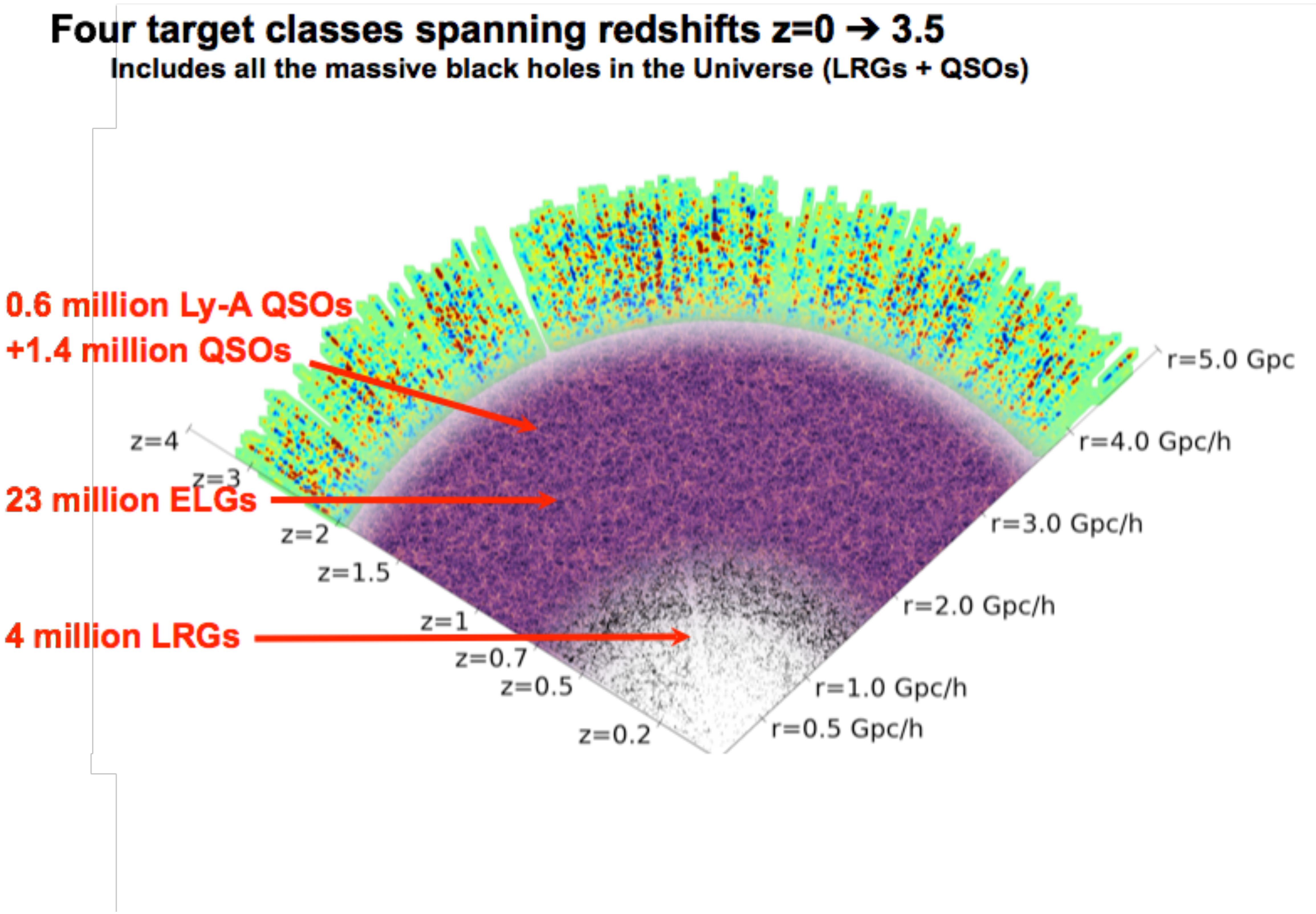

Precision & Accuracy

The measurement of growth function is improved up to the limit of shot noise about k_{max}<0.15h/Mpc

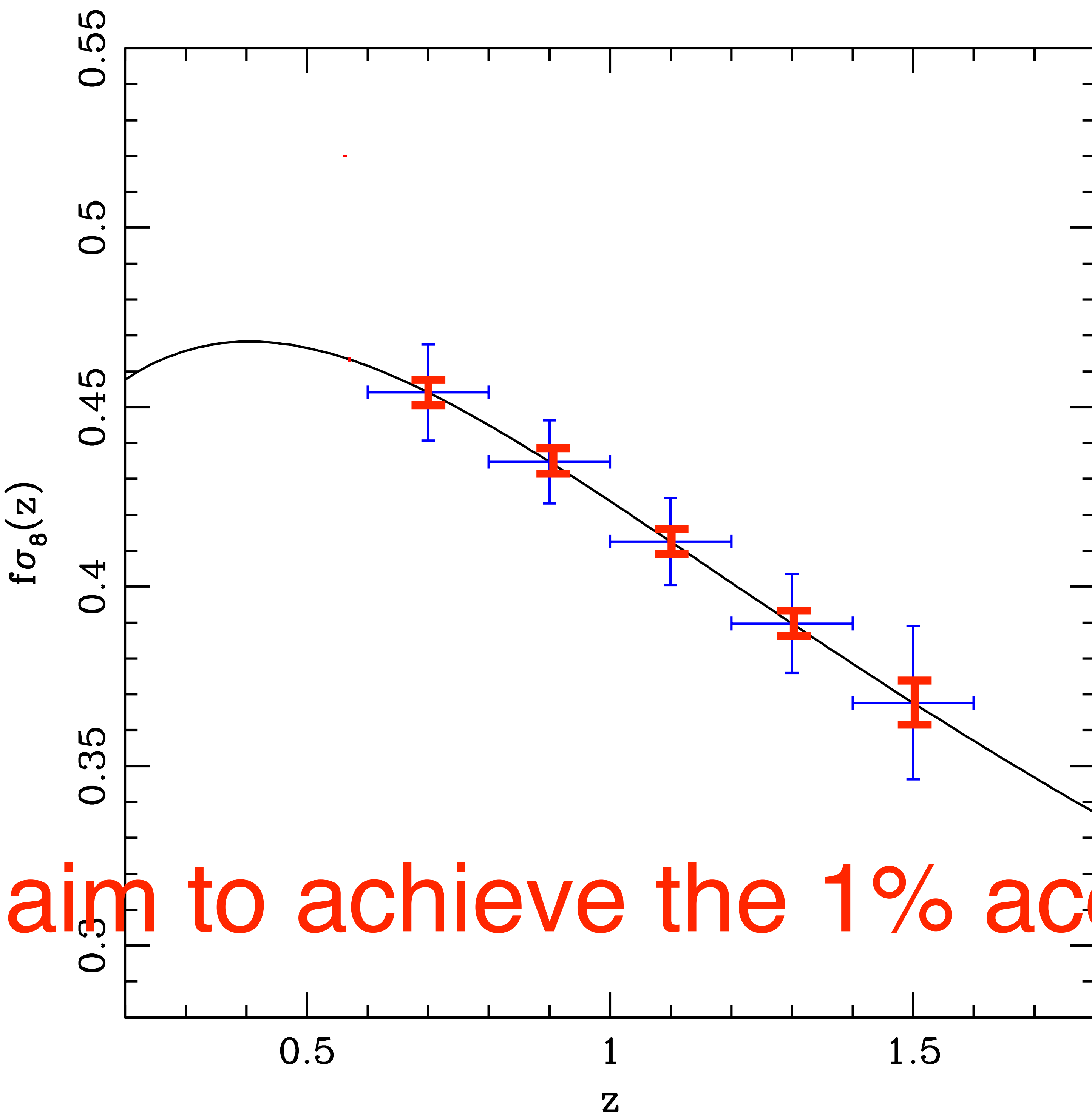

We aim to achieve the 1% accuracy

Open new window to test cosmological models

(D_A, H^{-1}, G_δ, G_Θ, FoG)

Standard model

Cold dark matter

Massless neutrino

New physics

Quintessence dark energy

Phantom dark energy

Λ

Open new window to test cosmological models

(D_A, H^{-1}, G_δ, G_Θ, FoG, New, New, …)

Standard model

Cold dark matter

Massless neutrino

Hot or warm dark matter

Massive neutrino

Interacting dark matter

Unified dark matter

Λ

New physics

Quintessence dark energy

Phantom dark energy

Decaying vacuum

Chameleon type gravity

Dilaton or Symmetron

Vainstein type gravity

Inhomogeneity of universe

non-Friedman universe

Precise determination on Ω_Λ

(D_A, H^{-1}, G_δ, G_Θ, FoG)

Standard model

Cold dark matter

Massless neutrino

Λ

The measured spectra with different Ω_Λ

We vary Ω_Λ coherently with BAO statistics, i.e. the observed sound horizon is fixed

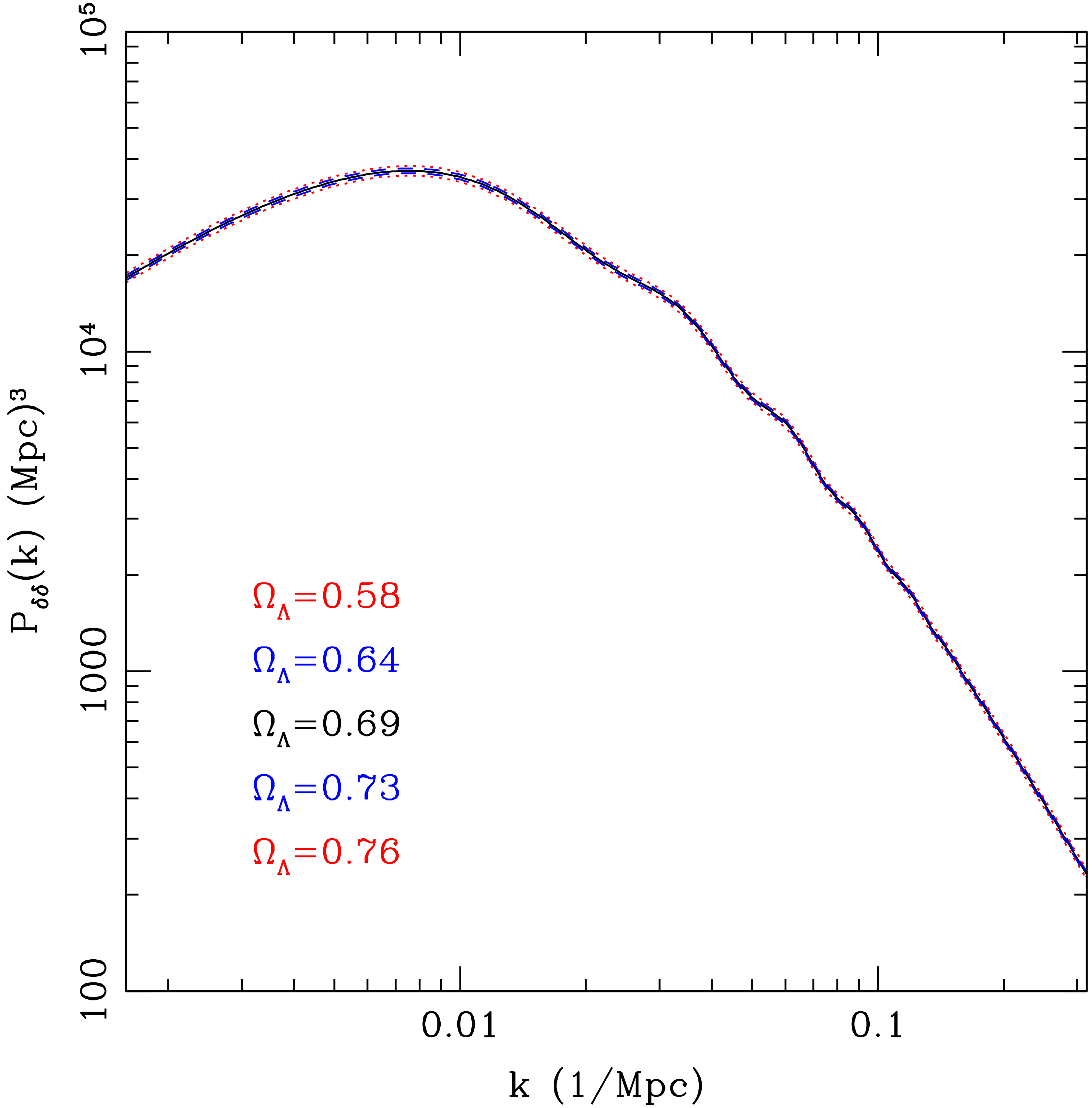

Mapping of clustering from real to redshift spaces

$$P_s(k,\boldsymbol{\mu}) = \int d^3x\, e^{ikx} \langle \boldsymbol{\delta\delta} \rangle$$

$$\Downarrow$$

$$P_s(k,\mu) = \int d^3x\, e^{ikx} \langle e^{jv} (\boldsymbol{\delta}+\boldsymbol{\mu}^2\Theta)(\boldsymbol{\delta}+\boldsymbol{\mu}^2\Theta) \rangle$$

$$= \int d^3x\, e^{ikx} \exp\{\langle e^{jv}\rangle_c\} \left[\langle e^{jv}(\boldsymbol{\delta}+\boldsymbol{\mu}^2\Theta)(\boldsymbol{\delta}+\boldsymbol{\mu}^2\Theta)\rangle_c + \langle e^{jv}(\boldsymbol{\delta}+\boldsymbol{\mu}^2\Theta)\rangle_c \langle e^{jv}(\boldsymbol{\delta}+\boldsymbol{\mu}^2\Theta)\rangle_c\right]$$

- Non-linear corrections: there is limit in the perturbative approach at smaller scales. We need find a way to combine the simulation result.
- Higher order polynomials: there is an infinite tower of cross correlation between velocity and density fields. We have to decide the order limit.
- The FoG effect: the exact functional form is unknown. Only thing that we know is that it is a function of velocity dispersion σ_p.

The nonlinear physics contamination

The discrepancy between linear prediction and measurement

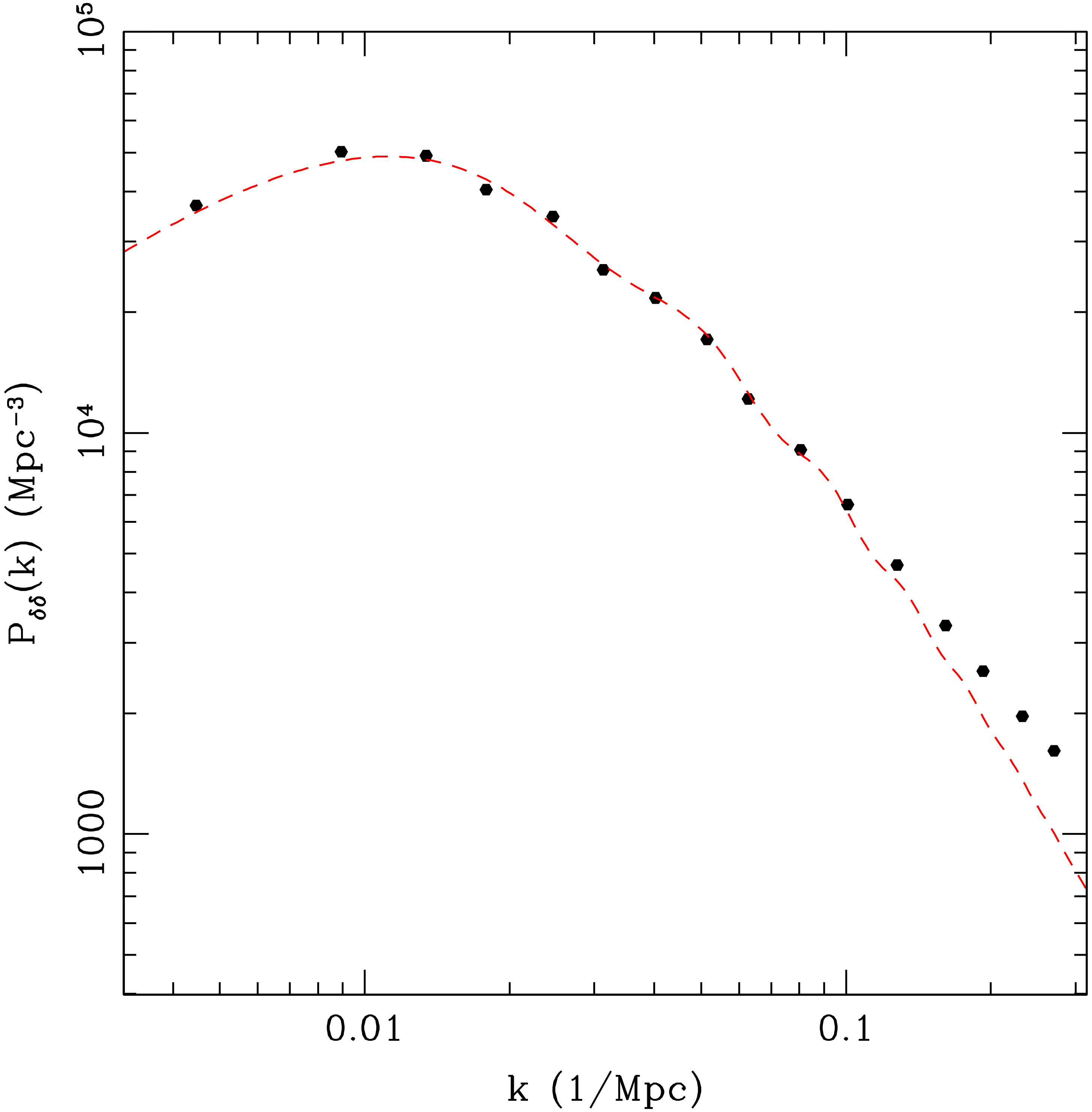

The nonlinear physics contamination

Theoretical prediction is improved by perturbation theory by two loop corrections

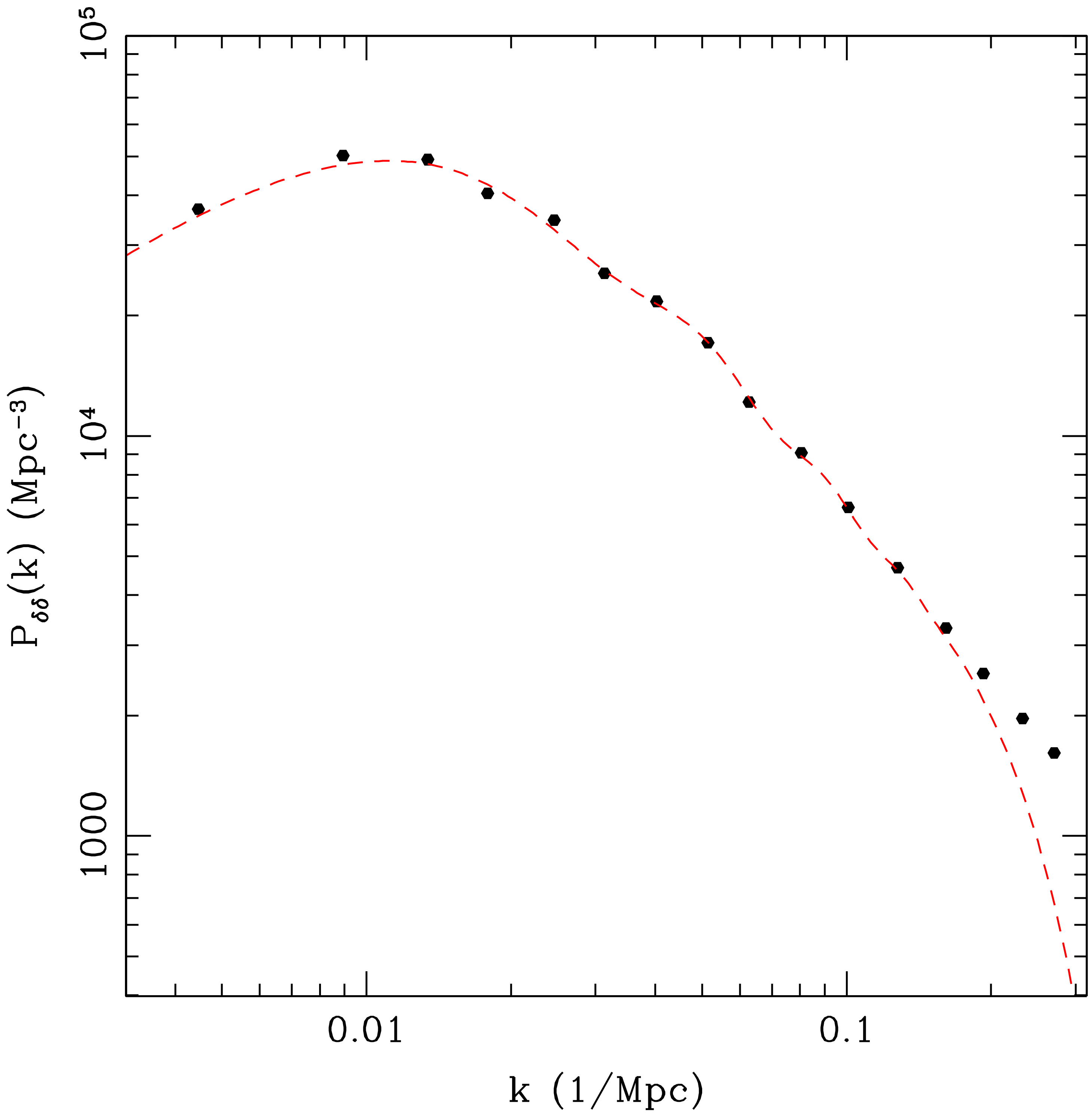

The estimated density-density spectrum

We estimate the power spectrum with the fixed fiducial template

$$
\begin{aligned}
\bar{P}_{XY}(k,z) &= \bar{\Gamma}^{(1)}_X(k,z)\bar{\Gamma}^{(1)}_Y(k,z)\bar{P}^i_{XY}(k) \\
&+2\int \frac{d^3\vec{q}}{(2\pi)^3}\bar{\Gamma}^{(2)}_X(\vec{q},\vec{k}-\vec{q},z)\bar{\Gamma}^{(2)}_Y(\vec{q},\vec{k}-\vec{q},z)\bar{P}^i_{XY}(q)\bar{P}^i_{XY}(|\vec{k}-\vec{q}|) \\
&+6\int \frac{d^3\vec{p}d^3\vec{q}}{(2\pi)^6}\bar{\Gamma}^{(3)}_X(\vec{p},\vec{q},\vec{k}-\vec{p}-\vec{q},z)\bar{\Gamma}^{(3)}_Y(\vec{p},\vec{q},\vec{k}-\vec{p}-\vec{q},z)\bar{P}^i_{XY}(p)\bar{P}^i_{XY}(q)\bar{P}^i_{XY}(|\vec{k}-\vec{p}-\vec{q}|)
\end{aligned}
$$

$$
\bar{\Gamma}^{(1)}_X(k,z) = \exp(-\bar{\gamma})\sum_n \bar{G}^n_X \bar{\mathcal{C}}^{(1)}_n(\bar{\gamma})
$$

$$
\begin{aligned}
\bar{\mathcal{C}}^{(1)}_1(\bar{\gamma}) &= 1 \\
\bar{\mathcal{C}}^{(1)}_3(\bar{\gamma}) &= \bar{\gamma} + \bar{\Gamma}^{(1)}_{X,1-\mathrm{loop}}(k) \\
\bar{\mathcal{C}}^{(1)}_5(\bar{\gamma}) &= \bar{\gamma}^2/2 + \bar{\gamma}\bar{\Gamma}^{(1)}_{X,1-\mathrm{loop}}(k) + \bar{\Gamma}^{(1)}_{X,2-\mathrm{loop}}(k) + \bar{\mathcal{O}}^{(1)}_{X,5} \\
\bar{\mathcal{C}}^{(1)}_n(\bar{\gamma}) &= \bar{\mathcal{O}}^{(1)}_{X,n}
\end{aligned}
$$

The estimated density-density spectrum

We estimate the power spectrum with the fixed fiducial template

$$
\begin{aligned}
&\bar{P}_{XY}(k,z) = \bar{\Gamma}^{(1)}_X(k,z)\bar{\Gamma}^{(1)}_Y(k,z)\bar{P}^i_{XY}(k) \\
&+2\int \frac{d^3\vec{q}}{(2\pi)^3}\bar{\Gamma}^{(2)}_X(\vec{q},\vec{k}-\vec{q},z)\bar{\Gamma}^{(2)}_Y(\vec{q},\vec{k}-\vec{q},z)\bar{P}^i_{XY}(q)\bar{P}^i_{XY}(|\vec{k}-\vec{q}|) \\
&+6\int \frac{d^3\vec{p}d^3\vec{q}}{(2\pi)^6}\bar{\Gamma}^{(3)}_X(\vec{p},\vec{q},\vec{k}-\vec{p}-\vec{q},z)\bar{\Gamma}^{(3)}_Y(\vec{p},\vec{q},\vec{k}-\vec{p}-\vec{q},z)\bar{P}^i_{XY}(p)\bar{P}^i_{XY}(q)\bar{P}^i_{XY}(|\vec{k}-\vec{p}-\vec{q}|)
\end{aligned}
$$

$$
\begin{aligned}
\bar{\Gamma}^{(2)}_X(k,z) &= \exp(-\bar{\gamma})\sum_n \bar{G}^n_X \bar{\mathcal{C}}^{(2)}_n \\
\bar{\mathcal{C}}^{(2)}_2(\bar{\gamma}) &= \bar{F}^{(2)}_X(\vec{q},\vec{k}-\vec{q}) \\
\bar{\mathcal{C}}^{(2)}_4(\bar{\gamma}) &= \frac{\bar{\gamma}}{2}\bar{F}^{(2)}_X(\vec{q},\vec{k}-\vec{q}) + \bar{\Gamma}^{(2)}_{X,1\text{-loop}}(\vec{q},\vec{k}-\vec{q}) + \bar{\mathcal{O}}^{(2)}_{X,4} \\
\bar{\mathcal{C}}^{(2)}_n(\bar{\gamma}) &= \bar{\mathcal{O}}^{(2)}_{X,n}
\end{aligned}
$$

The estimated density-density spectrum

We estimate the power spectrum with the fixed fiducial template

$$
\begin{aligned}
&\bar{P}_{XY}(k,z) = \bar{\Gamma}^{(1)}_X(k,z)\bar{\Gamma}^{(1)}_Y(k,z)\bar{P}^i_{XY}(k) \\
&+2\int \frac{d^3\vec{q}}{(2\pi)^3}\bar{\Gamma}^{(2)}_X(\vec{q},\vec{k}-\vec{q},z)\bar{\Gamma}^{(2)}_Y(\vec{q},\vec{k}-\vec{q},z)\bar{P}^i_{XY}(q)\bar{P}^i_{XY}(|\vec{k}-\vec{q}|) \\
&+6\int \frac{d^3\vec{p}d^3\vec{q}}{(2\pi)^6}\bar{\Gamma}^{(3)}_X(\vec{p},\vec{q},\vec{k}-\vec{p}-\vec{q},z)\bar{\Gamma}^{(3)}_Y(\vec{p},\vec{q},\vec{k}-\vec{p}-\vec{q},z)\bar{P}^i_{XY}(p)\bar{P}^i_{XY}(q)\bar{P}^i_{XY}(|\vec{k}-\vec{p}-\vec{q}|)
\end{aligned}
$$

$$
\begin{aligned}
\bar{\Gamma}^{(3)}_X(k,z) &= \exp(-\gamma)\sum_n \bar{G}^n_X\bar{\mathcal{C}}^{(3)}_n \\
\bar{\mathcal{C}}^{(3)}_3(\bar{\gamma}) &= \bar{F}^{(3)}_X(\vec{p},\vec{q},\vec{k}-\vec{p}-\vec{q}) + \bar{\mathcal{O}}^{(3)}_{X,3} \\
\bar{\mathcal{C}}^{(3)}_n(\bar{\gamma}) &= \bar{\mathcal{O}}^{(3)}_{X,n}
\end{aligned}
$$

The estimated density-density spectrum

We estimate the power spectrum with the fixed fiducial template

$$
\begin{aligned}
&\bar{P}_{XY}(k,z) = \bar{\Gamma}^{(1)}_X(k,z)\bar{\Gamma}^{(1)}_Y(k,z)\bar{P}^i_{XY}(k) \\
&+2\int \frac{d^3\vec{q}}{(2\pi)^3}\bar{\Gamma}^{(2)}_X(\vec{q},\vec{k}-\vec{q},z)\bar{\Gamma}^{(2)}_Y(\vec{q},\vec{k}-\vec{q},z)\bar{P}^i_{XY}(q)\bar{P}^i_{XY}(|\vec{k}-\vec{q}|) \\
&+6\int \frac{d^3\vec{p}d^3\vec{q}}{(2\pi)^6}\bar{\Gamma}^{(3)}_X(\vec{p},\vec{q},\vec{k}-\vec{p}-\vec{q},z)\bar{\Gamma}^{(3)}_Y(\vec{p},\vec{q},\vec{k}-\vec{p}-\vec{q},z)\bar{P}^i_{XY}(p)\bar{P}^i_{XY}(q)\bar{P}^i_{XY}(|\vec{k}-\vec{p}-\vec{q}|)
\end{aligned}
$$

$$\bar{P}_{XY}(k,z) = \bar{P}^{\rm th}_{XY}(k,z) + \bar{P}^{\rm res}_{XY}(k,z)$$

$$
\begin{aligned}
&\bar{P}^{\rm res}_{XY} = \bar{G}_X\left[\bar{G}^5_Y\bar{\mathcal{O}}^{(1)}_{Y,5} + \text{higher}\right]\bar{P}^i_{XY} + \bar{G}_Y\left[\bar{G}^5_X\bar{\mathcal{O}}^{(1)}_{X,5} + \text{higher}\right]\bar{P}^i_{XY} \\
&+\bar{G}^2_X\int\left[\bar{G}^4_Y\bar{\mathcal{O}}^{(2)}_{Y,4}\bar{F}^{(2)}_Y + \text{higher}\right]\bar{P}^i_{XY}\bar{P}^i_{XY} + \bar{G}^2_Y\int\left[\bar{G}^4_X\bar{\mathcal{O}}^{(2)}_{X,4}\bar{F}^{(2)}_X + \text{higher}\right]\bar{P}^i_{XY}\bar{P}^i_{XY} \\
&+\bar{G}^3_X\int\int\left[\bar{G}^3_Y\bar{\mathcal{O}}^{(3)}_{Y,3}\bar{F}^{(3)}_Y + \text{higher}\right]\bar{P}^i_{XY}\bar{P}^i_{XY}\bar{P}^i_{XY} + \bar{G}^3_Y\int\int\left[\bar{G}^3_X\bar{\mathcal{O}}^{(3)}_{X,3}\bar{F}^{(3)}_X + \text{higher}\right]\bar{P}^i_{XY}\bar{P}^i_{XY}\bar{P}^i_{XY}
\end{aligned}
$$

The estimated density-density spectrum

Power spectrum in different cosmology is precisely reproduced

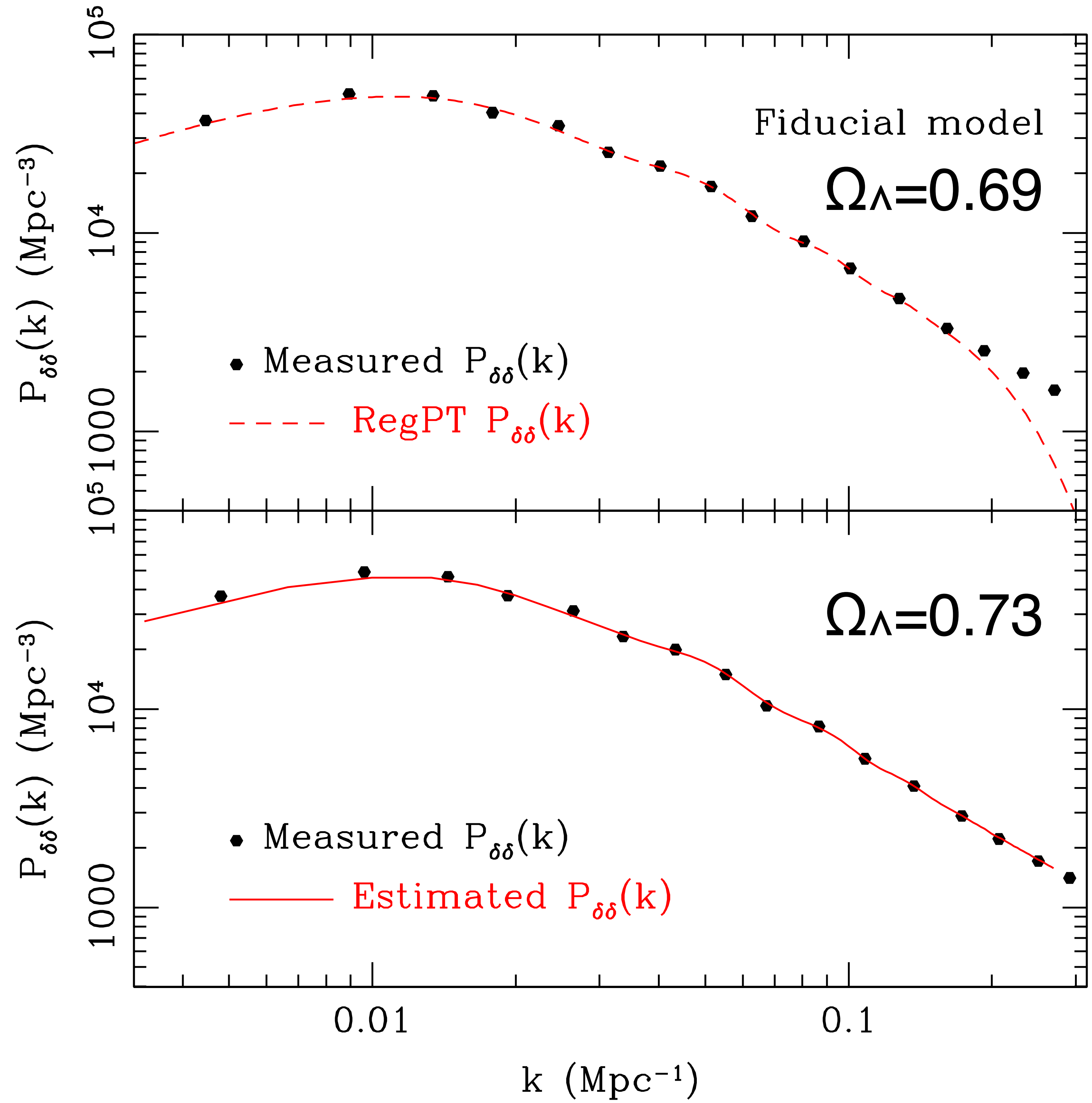

The fractional errors of estimation

Power spectrum in different cosmology is precisely reproduced

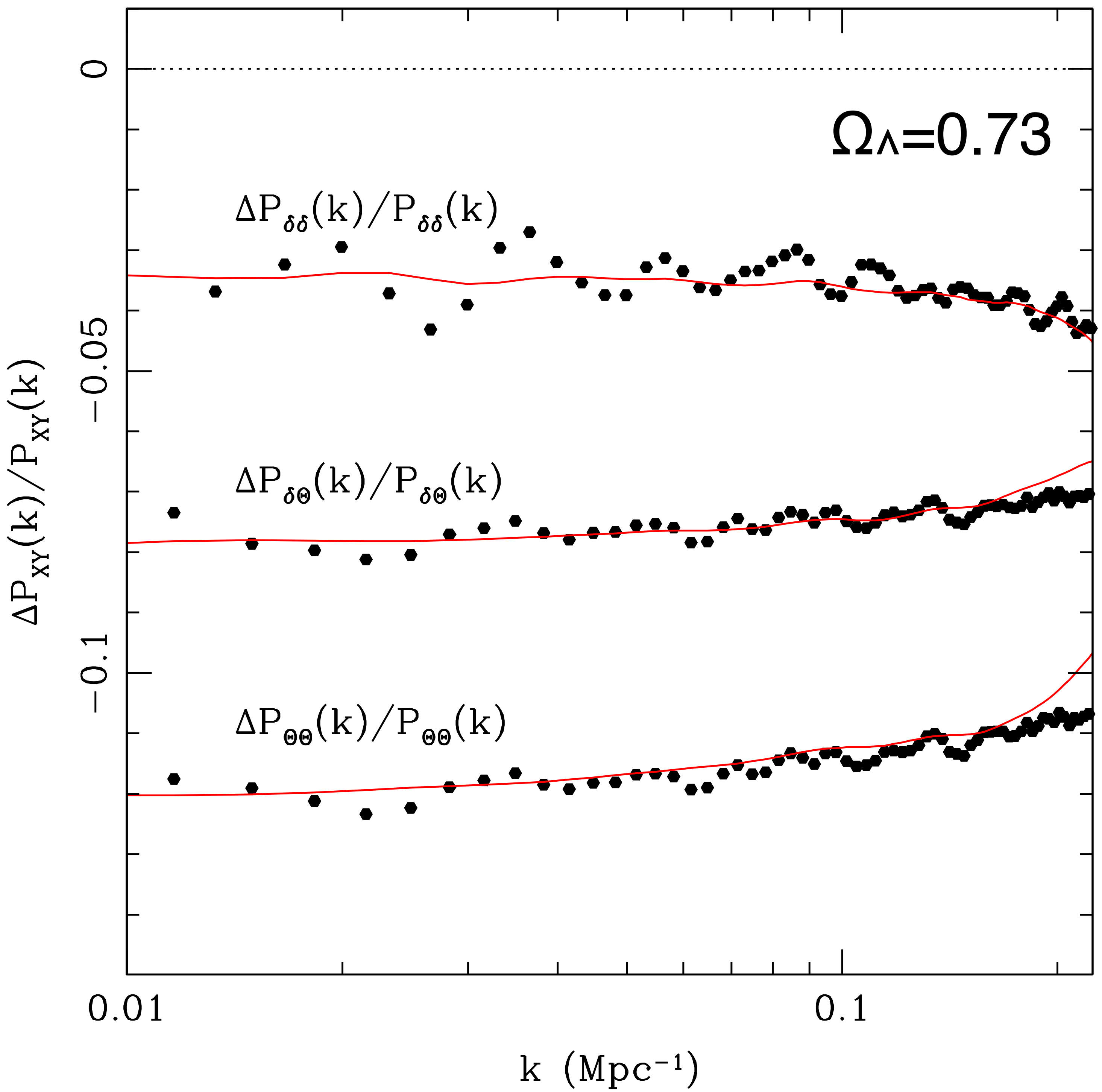

Mapping of clustering from real to redshift spaces

$$P_s(k,\boldsymbol{\mu}) = \int d^3x\, e^{ikx} \langle \boldsymbol{\delta\delta} \rangle$$

$$\Downarrow$$

$$P_s(k,\mu) = \int d^3x\, e^{ikx} \langle e^{jv} (\boldsymbol{\delta}+\boldsymbol{\mu}^2\Theta)(\boldsymbol{\delta}+\boldsymbol{\mu}^2\Theta) \rangle$$

$$= \int d^3x\, e^{ikx} \exp\{\langle e^{jv}\rangle_c\} \, [\langle e^{jv}(\boldsymbol{\delta}+\boldsymbol{\mu}^2\Theta)(\boldsymbol{\delta}+\boldsymbol{\mu}^2\Theta)\rangle_c + \langle e^{jv}(\boldsymbol{\delta}+\boldsymbol{\mu}^2\Theta)\rangle_c \langle e^{jv}(\boldsymbol{\delta}+\boldsymbol{\mu}^2\Theta)\rangle_c]$$

- Non-linear corrections: there is limit in the perturbative approach at smaller scales. We need find a way to combine the simulation result.
- Higher order polynomials: there is an infinite tower of cross correlation between velocity and density fields. We have to decide the order limit.
- The FoG effect: the exact functional form is unknown. Only thing that we know is that it is a function of velocity dispersion σ_p.

The estimated A

$$\bar{A}(k,\mu) = j_1 \int d^3\boldsymbol{x}\; e^{i\boldsymbol{k}\cdot\boldsymbol{x}} \langle A_1 A_2 A_3 \rangle_c = \sum_{n=1}^{6} \bar{A}_n$$

$$\bar{A}_1 = 2j_1 \int d^3\boldsymbol{x}\; e^{i\boldsymbol{k}\cdot\boldsymbol{x}} \langle \bar{u}_z(\boldsymbol{r})\bar{\delta}(\boldsymbol{r})\bar{\delta}(\boldsymbol{r}')\rangle_c$$

$$\bar{A}_2 = j_1 \int d^3\boldsymbol{x}\; e^{i\boldsymbol{k}\cdot\boldsymbol{x}} \langle u_z(\boldsymbol{r})\delta(\boldsymbol{r})\,\nabla_z u_z(\boldsymbol{r}')\rangle_c$$

$$\bar{A}_3 = j_1 \int d^3\boldsymbol{x}\; e^{i\boldsymbol{k}\cdot\boldsymbol{x}} \langle u_z(\boldsymbol{r})\,\nabla_z u_z(\boldsymbol{r})\delta(\boldsymbol{r}')\rangle_c$$

$$\bar{A}_4 = 2j_1 \int d^3\boldsymbol{x}\; e^{i\boldsymbol{k}\cdot\boldsymbol{x}} \langle u_z(\boldsymbol{r})\,\nabla_z u_z(\boldsymbol{r})\,\nabla_z u_z(\boldsymbol{r}')\rangle_c$$

$$\bar{A}_5 = j_1 \int d^3\boldsymbol{x}\; e^{i\boldsymbol{k}\cdot\boldsymbol{x}} \langle -\delta(\boldsymbol{r})u_z(\boldsymbol{r}')\,\nabla_z u_z(\boldsymbol{r}')\rangle_c$$

$$\bar{A}_6 = j_1 \int d^3\boldsymbol{x}\; e^{i\boldsymbol{k}\cdot\boldsymbol{x}} \langle -\nabla_z u_z(\boldsymbol{r})u_z(\boldsymbol{r}')\delta(\boldsymbol{r}')\rangle_c$$

$$\begin{aligned}
\bar{A}(k,\mu) &= \sum_{n=1}^{6} \mathcal{A}_n \\
&= \left(G_\delta/\bar{G}_\delta\right)^2 \left(G_\Theta/\bar{G}_\Theta\right) \bar{A}_1 + \left(G_\delta/\bar{G}_\delta\right) \left(G_\Theta/\bar{G}_\Theta\right)^2 \bar{A}_2 \\
&+ \left(G_\delta/\bar{G}_\delta\right) \left(G_\Theta/\bar{G}_\Theta\right)^2 \bar{A}_3 + \left(G_\Theta/\bar{G}_\Theta\right)^3 \bar{A}_4 \\
&+ \left(G_\delta/\bar{G}_\delta\right) \left(G_\Theta/\bar{G}_\Theta\right)^2 \bar{A}_5 + \left(G_\delta/\bar{G}_\delta\right) \left(G_\Theta/\bar{G}_\Theta\right)^2 \bar{A}_6
\end{aligned}$$

The estimated A

Higher order polynomial A is precisely reproduced

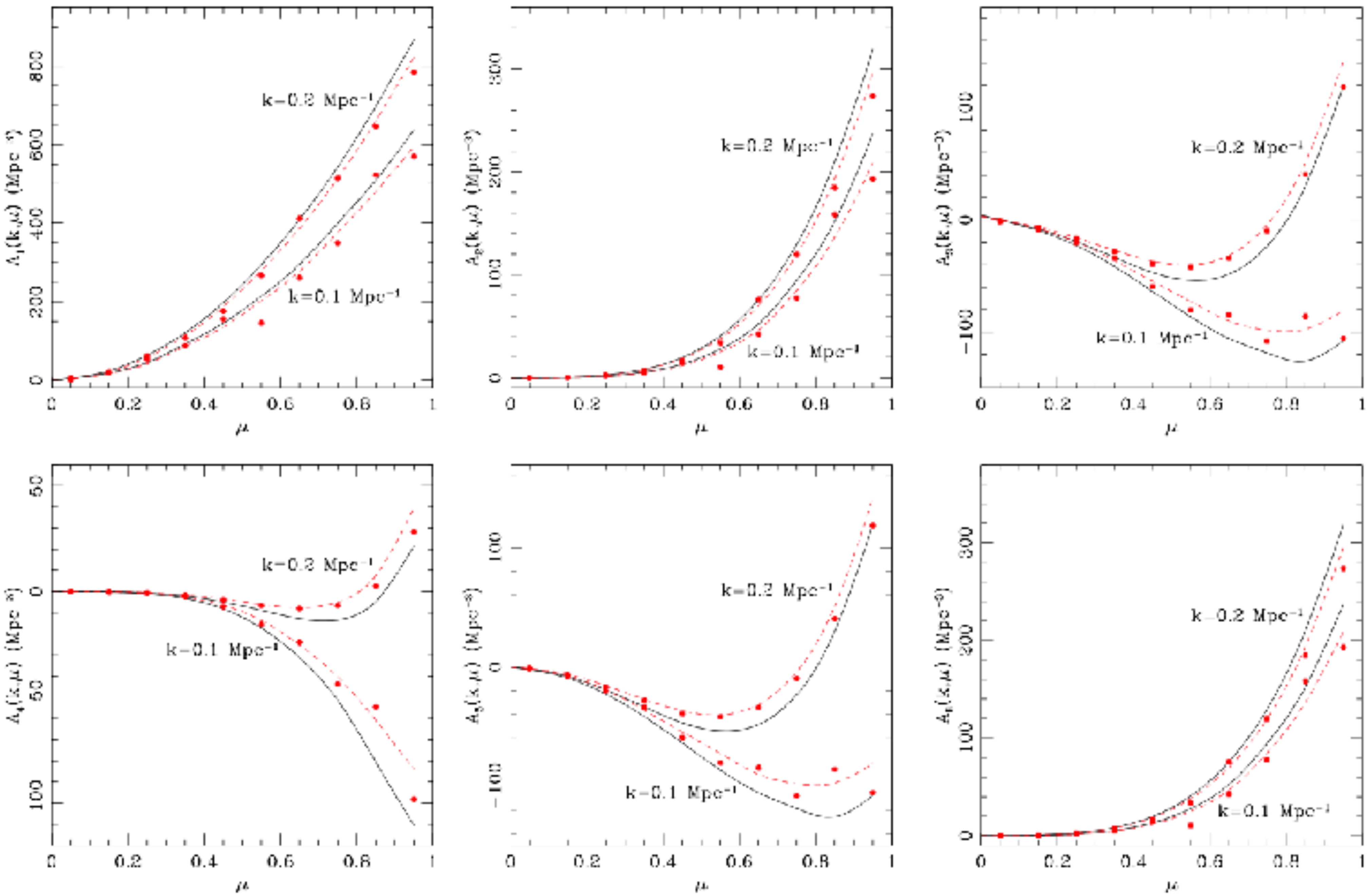

The estimated B

$$\bar{B}(k,\mu) = j_1^2 \int d^3\boldsymbol{x}\; e^{i\boldsymbol{k}\cdot\boldsymbol{x}}\; \langle A_1 A_2\rangle_c \langle A_1 A_3\rangle_c$$
$$= \sum_{n=1}^{4} \bar{\mathcal{B}}_n$$

$$\bar{\mathcal{B}}_1 = j_1^2 \int d^3\boldsymbol{x}\; e^{i\boldsymbol{k}\cdot\boldsymbol{x}}\; \langle -u_z(\boldsymbol{r}')\delta(\boldsymbol{r})\rangle_c \langle u_z(\boldsymbol{r})\delta(\boldsymbol{r}')\rangle_c$$
$$\bar{\mathcal{B}}_2 = j_1^2 \int d^3\boldsymbol{x}\; e^{i\boldsymbol{k}\cdot\boldsymbol{x}}\; \langle -u_z(\boldsymbol{r}')\delta(\boldsymbol{r})\rangle_c \langle u_z(\boldsymbol{r})\,\nabla_z u_z(\boldsymbol{r}')\rangle_c$$
$$\bar{\mathcal{B}}_3 = j_1^2 \int d^3\boldsymbol{x}\; e^{i\boldsymbol{k}\cdot\boldsymbol{x}}\; \langle -u_z(\boldsymbol{r}')\,\nabla_z u_z(\boldsymbol{r})\rangle_c \langle u_z(\boldsymbol{r})\delta(\boldsymbol{r}')\rangle_c$$
$$\bar{\mathcal{B}}_4 = j_1^2 \int d^3\boldsymbol{x}\; e^{i\boldsymbol{k}\cdot\boldsymbol{x}}\; \langle -u_z(\boldsymbol{r}')\,\nabla_z u_z(\boldsymbol{r})\rangle_c \langle u_z(\boldsymbol{r})\,\nabla_z u_z(\boldsymbol{r}')\rangle_c$$

$$\bar{B}(k,\mu) = \sum_{n=1}^{4} \mathcal{B}_n$$
$$= \left(G_\delta/\bar{G}_\delta\right)^2 \left(G_\Theta/\bar{G}_\Theta\right)^2 \bar{\mathcal{B}}_1 + \left(G_\delta/\bar{G}_\delta\right) \left(G_\Theta/\bar{G}_\Theta\right)^3 \bar{\mathcal{B}}_2$$
$$+ \left(G_\delta/\bar{G}_\delta\right) \left(G_\Theta/\bar{G}_\Theta\right)^3 \bar{\mathcal{B}}_3 + \left(G_\Theta/\bar{G}_\Theta\right)^4 \bar{\mathcal{B}}_4$$

The estimated B

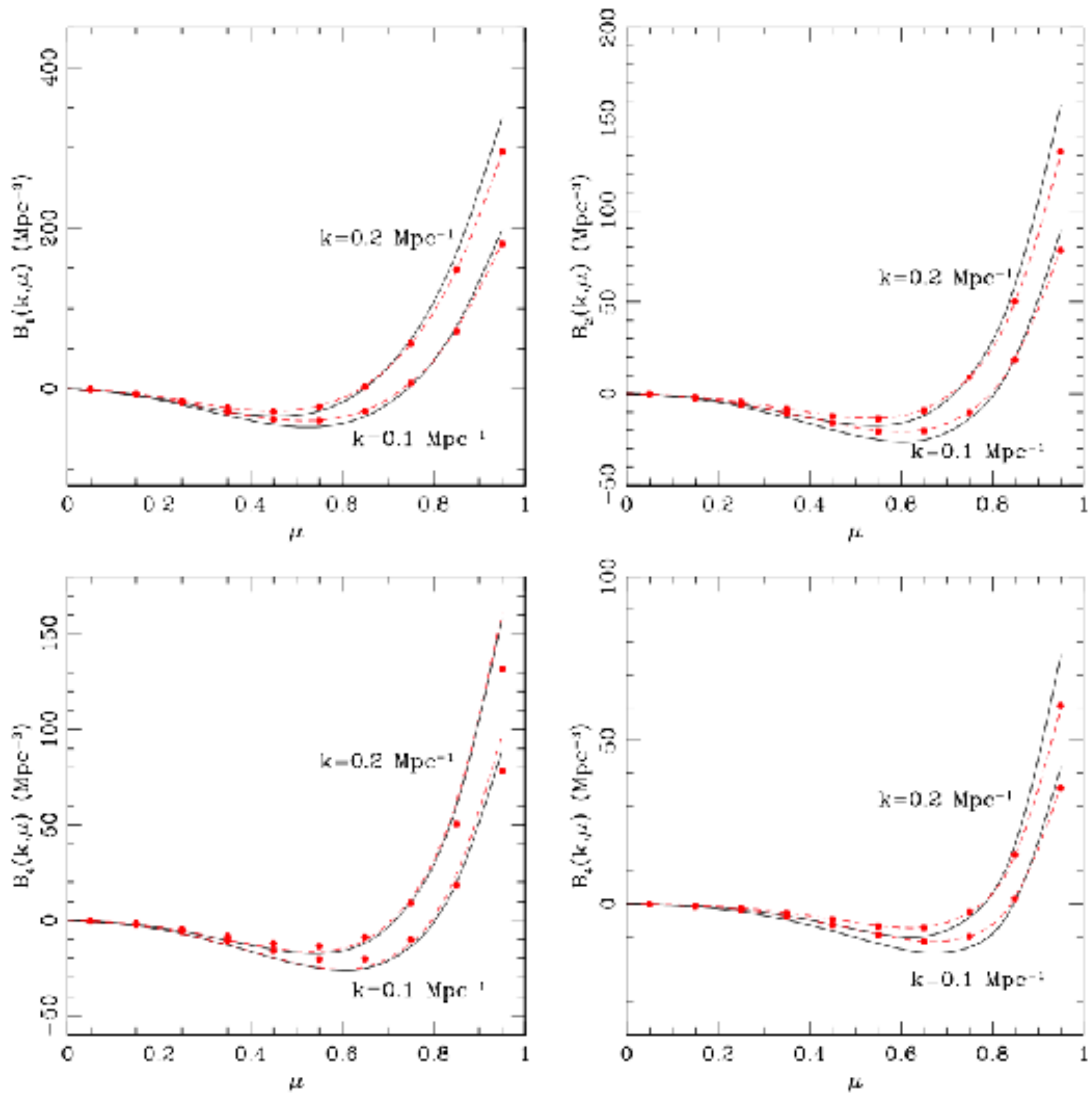

The estimated T

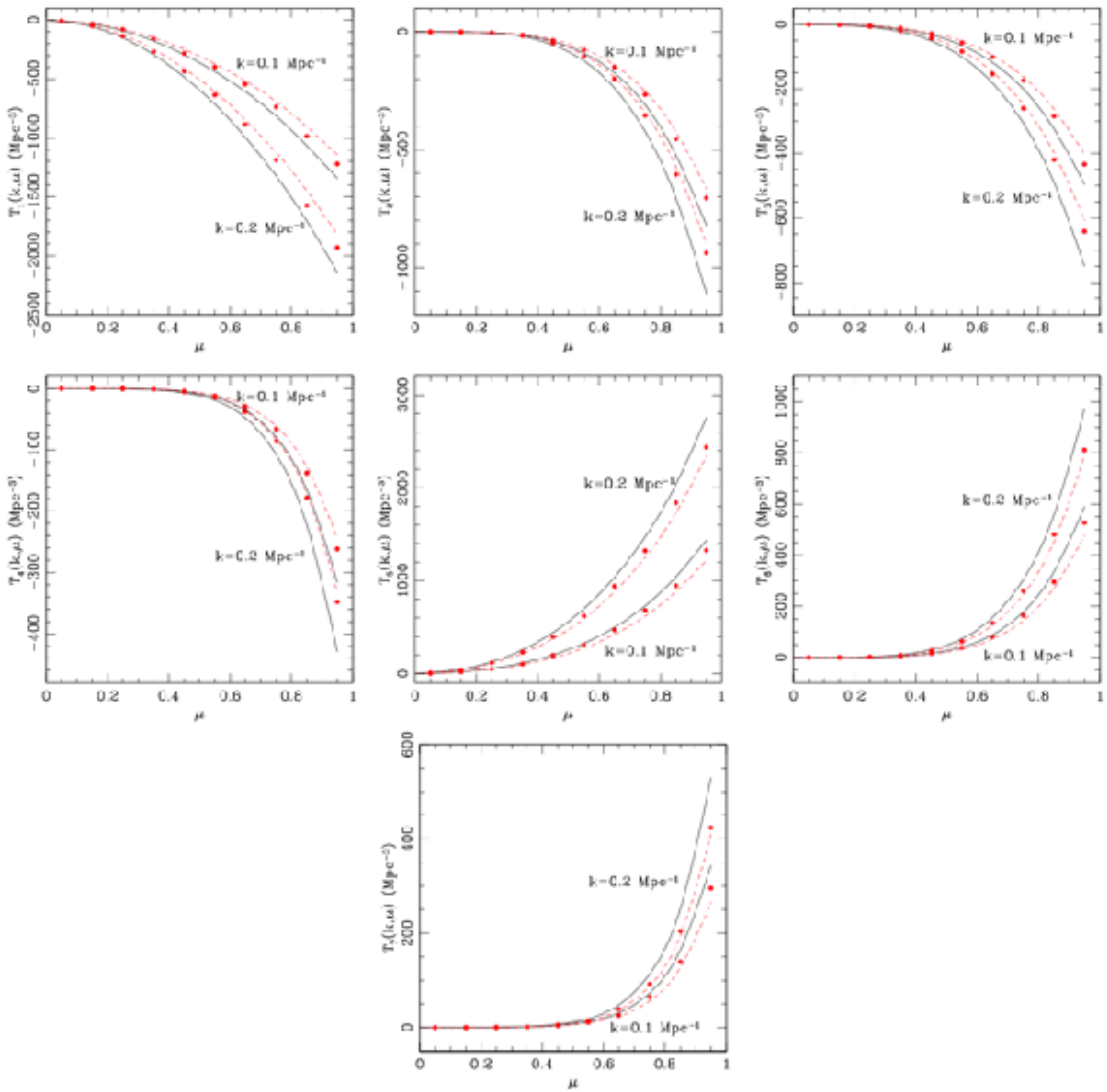

The estimated T

$$\bar{T}(k,\mu) = \frac{1}{2} j_1^2 \int d^3\boldsymbol{x}\; e^{i\boldsymbol{k}\cdot\boldsymbol{x}} \; \langle A_1^2 A_2 A_3 \rangle_c,$$
$$= \sum_{n=1}^{7} \bar{\mathcal{T}}_n$$

$$\bar{\mathcal{T}}_1 = j_1^2 \int d^3\boldsymbol{x}\; e^{i\boldsymbol{k}\cdot\boldsymbol{x}} \; \langle u_z(\boldsymbol{r}) u_z(\boldsymbol{r}) \delta(\boldsymbol{r}) \delta(\boldsymbol{r}') \rangle_c$$
$$\bar{\mathcal{T}}_2 = j_1^2 \int d^3\boldsymbol{x}\; e^{i\boldsymbol{k}\cdot\boldsymbol{x}} \; \langle u_z(\boldsymbol{r}) u_z(\boldsymbol{r}) \delta(\boldsymbol{r}) \, \nabla_z u_z(\boldsymbol{r}') \rangle_c$$
$$\bar{\mathcal{T}}_3 = j_1^2 \int d^3\boldsymbol{x}\; e^{i\boldsymbol{k}\cdot\boldsymbol{x}} \; \langle u_z(\boldsymbol{r}) u_z(\boldsymbol{r}) \, \nabla_z u_z(\boldsymbol{r}) \delta(\boldsymbol{r}') \rangle_c$$
$$\bar{\mathcal{T}}_4 = j_1^2 \int d^3\boldsymbol{x}\; e^{i\boldsymbol{k}\cdot\boldsymbol{x}} \; \langle u_z(\boldsymbol{r}) u_z(\boldsymbol{r}) \, \nabla_z u_z(\boldsymbol{r}) \, \nabla_z u_z(\boldsymbol{r}') \rangle_c$$
$$\bar{\mathcal{T}}_5 = \frac{1}{2} j_1^2 \int d^3\boldsymbol{x}\; e^{i\boldsymbol{k}\cdot\boldsymbol{x}} \; \langle -2 u_z(\boldsymbol{r}') u_z(\boldsymbol{r}) \delta(\boldsymbol{r}) \delta(\boldsymbol{r}') \rangle_c$$
$$\bar{\mathcal{T}}_6 = j_1^2 \int d^3\boldsymbol{x}\; e^{i\boldsymbol{k}\cdot\boldsymbol{x}} \; \langle -2 u_z(\boldsymbol{r}') u_z(\boldsymbol{r}) \delta(\boldsymbol{r}) \, \nabla_z u_z(\boldsymbol{r}') \rangle_c$$
$$\bar{\mathcal{T}}_7 = \frac{1}{2} j_1^2 \int d^3\boldsymbol{x}\; e^{i\boldsymbol{k}\cdot\boldsymbol{x}} \; \langle -2 u_z(\boldsymbol{r}') u_z(\boldsymbol{r}) \, \nabla_z u_z(\boldsymbol{r}) \, \nabla_z u_z(\boldsymbol{r}') \rangle_c$$

$$\begin{aligned} T(k,\mu) &= \sum_{n=1}^{3} \mathcal{T}_n \\ &= \left(G_\delta/\bar{G}_\delta\right)^2 \left(G_\Theta/\bar{G}_\Theta\right)^2 \bar{\mathcal{T}}_1 + \left(G_\delta/\bar{G}_\delta\right) \left(G_\Theta/\bar{G}_\Theta\right)^3 \bar{\mathcal{T}}_2 + \left(G_\delta/\bar{G}_\delta\right) \left(G_\Theta/\bar{G}_\Theta\right)^3 \bar{\mathcal{T}}_3 \\ &+ \left(G_\Theta/\bar{G}_\Theta\right)^4 \bar{\mathcal{T}}_4 + \left(G_\delta/\bar{G}_\delta\right)^2 \left(G_\Theta/\bar{G}_\Theta\right)^2 \bar{\mathcal{T}}_5 + \left(G_\delta/\bar{G}_\delta\right) \left(G_\Theta/\bar{G}_\Theta\right)^3 \bar{\mathcal{T}}_6 + \left(G_\Theta/\bar{G}_\Theta\right)^4 \bar{\mathcal{T}}_7 \end{aligned}$$

The accurate measurement of growth functions

We achieve the 1% accuracy measurement after a long journey through perturbation theory and simulation template

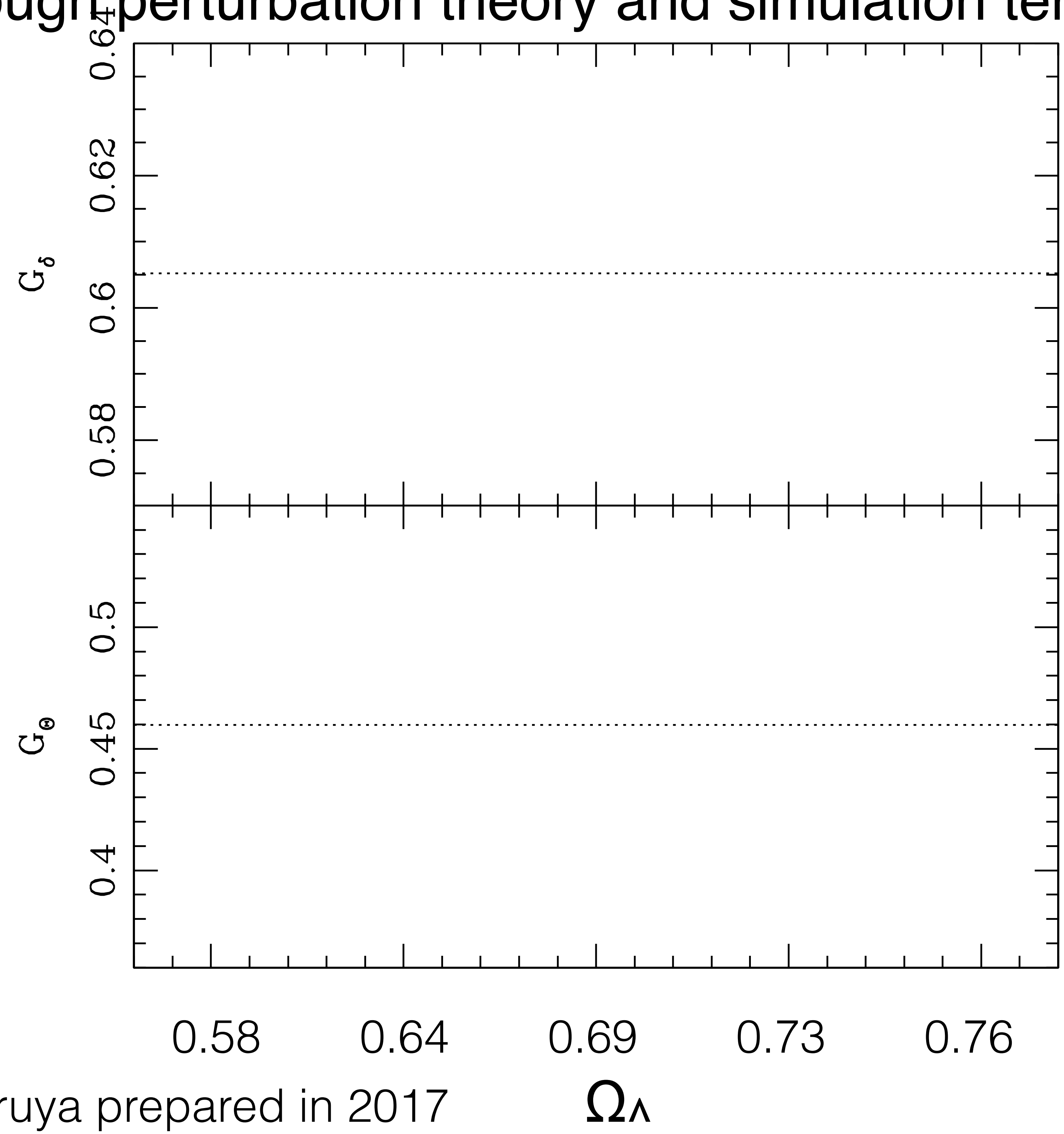

YSS, Yi, Oh and Taruya prepared in 2017

The accurate measurement of growth functions

We achieve the 1% accuracy measurement after a long journey through perturbation theory and simulation template

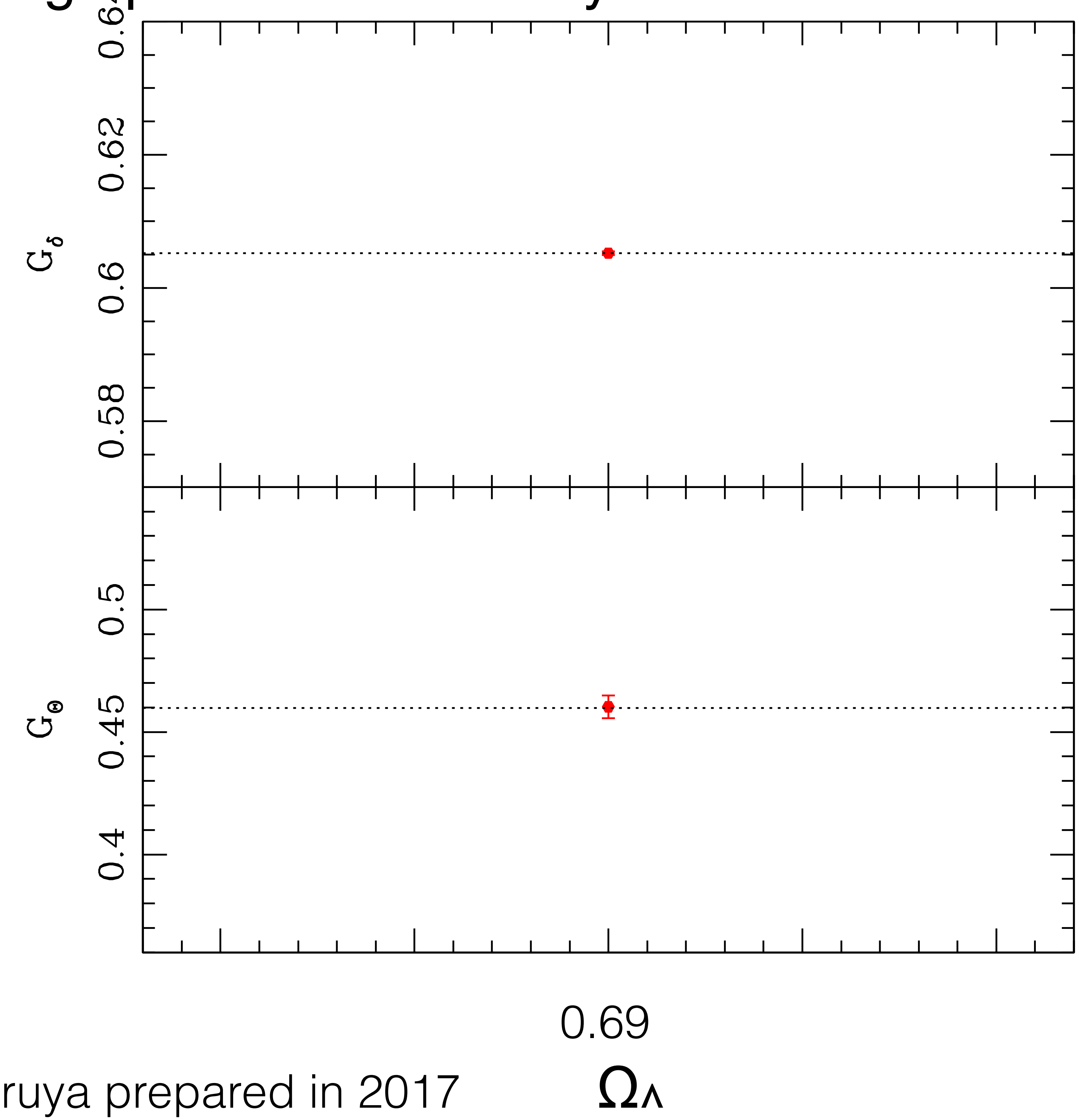

YSS, Yi, Oh and Taruya prepared in 2017

The accurate measurement of growth functions

We achieve the 1% accuracy measurement after a long journey through perturbation theory and simulation template

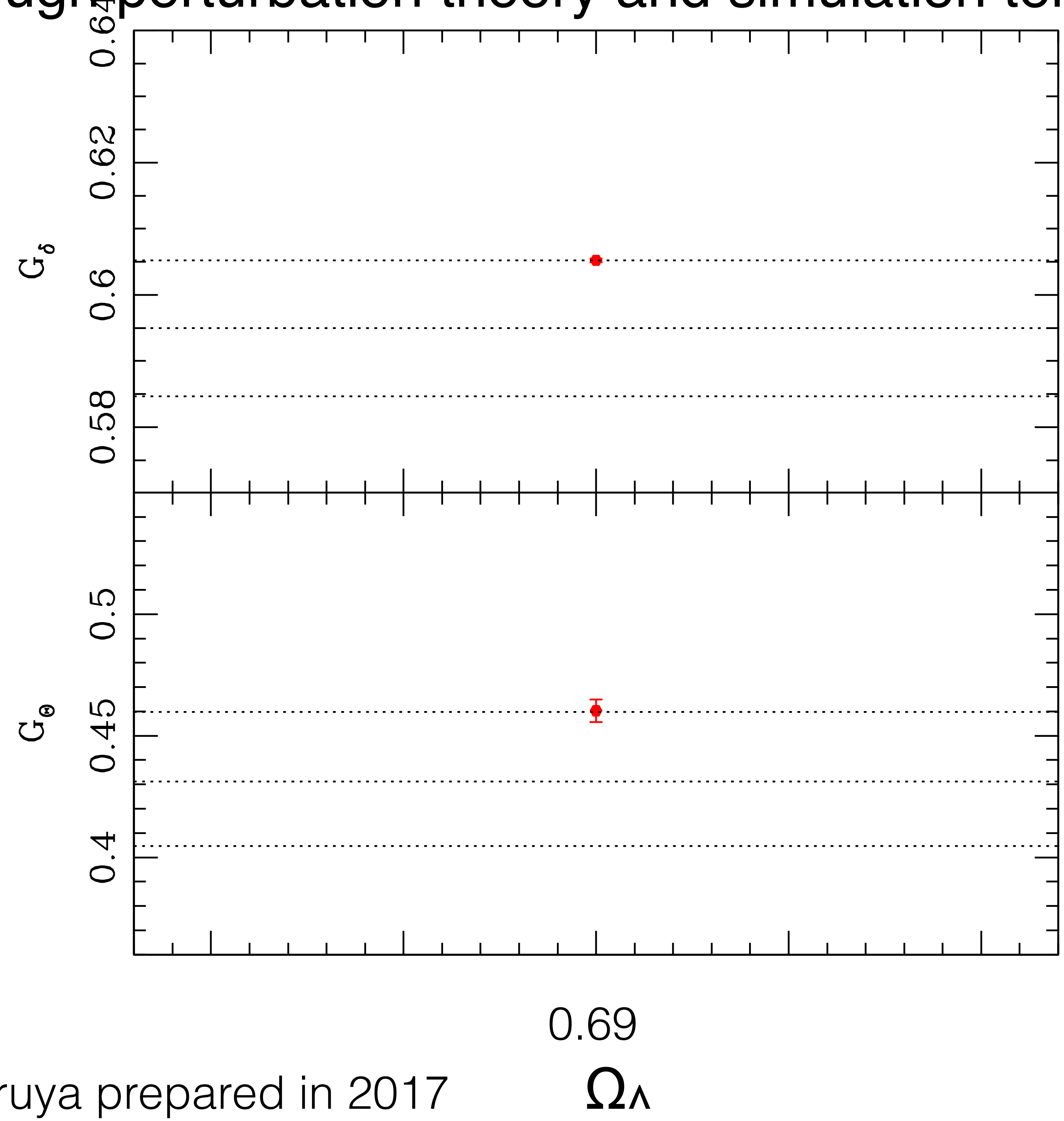

YSS, Yi, Oh and Taruya prepared in 2017

The accurate measurement of growth functions

We achieve the 1% accuracy measurement after a long journey through perturbation theory and simulation template

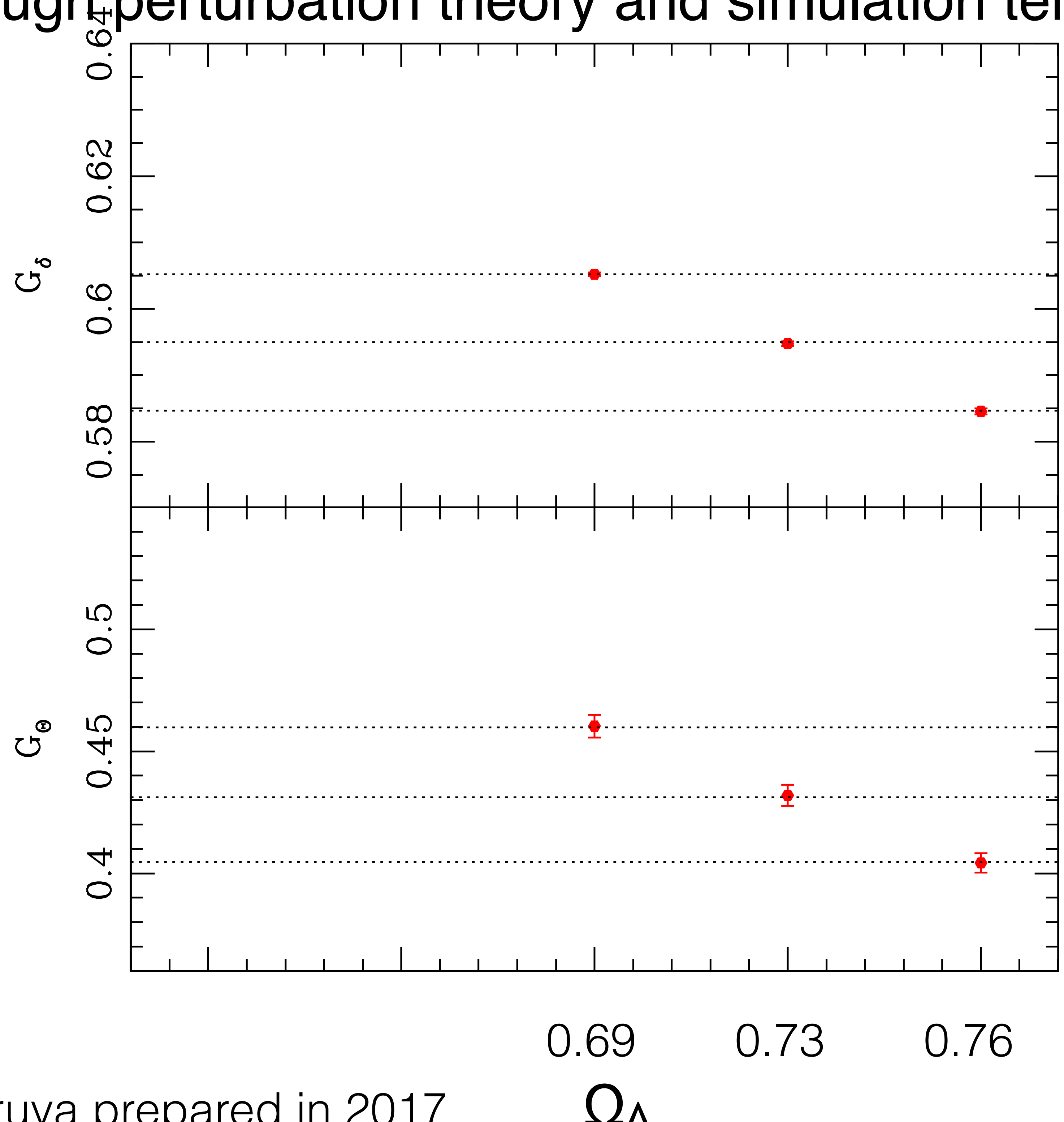

YSS, Yi, Oh and Taruya prepared in 2017

The accurate measurement of growth functions

We achieve the 1% accuracy measurement after a long journey through perturbation theory and simulation template

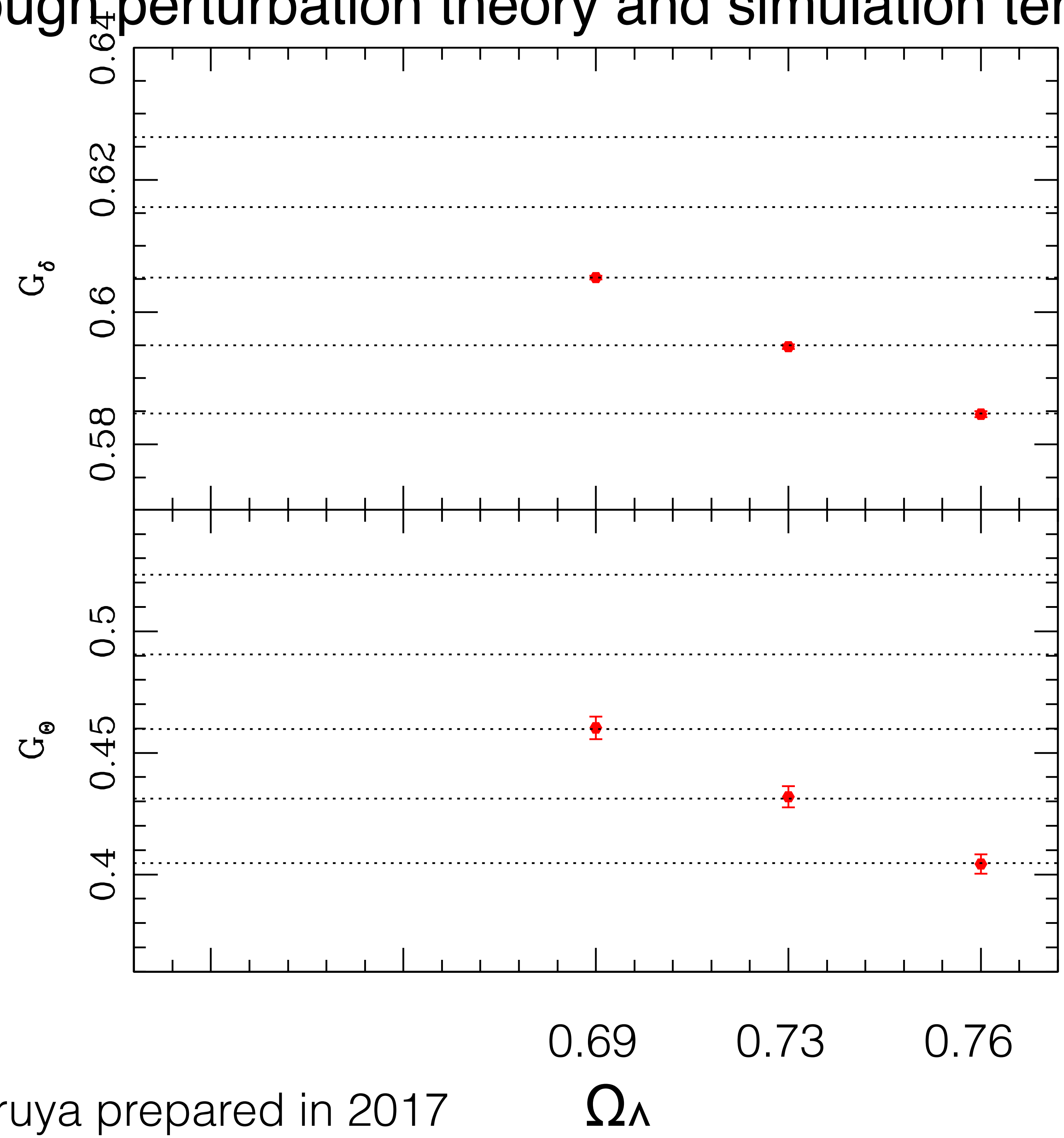

YSS, Yi, Oh and Taruya prepared in 2017

The accurate measurement of growth functions

We achieve the 1% accuracy measurement after a long journey through perturbation theory and simulation template

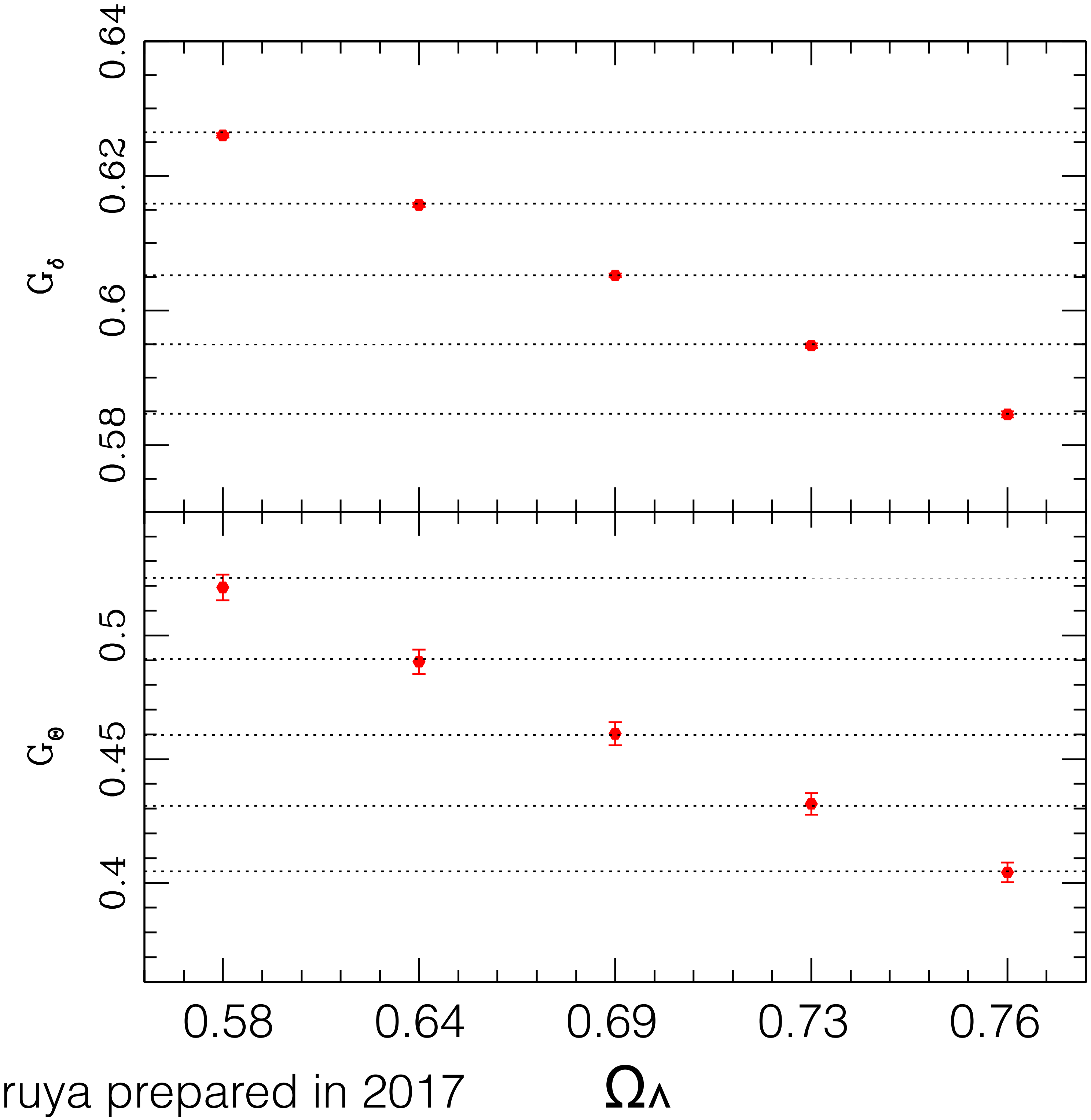

YSS, Yi, Oh and Taruya prepared in 2017

Precise determination on Ω_Λ

(D_A, H^{-1}, G_δ, G_Θ, FoG)

Standard model

Cold dark matter

Massless neutrino

Λ

Open new window to test cosmological models

(D_A, H^{-1}, G_δ, G_Θ, FoG)

Standard model

Cold dark matter

Massless neutrino

New physics

Quintessence dark energy

Phantom dark energy

Λ

Open new window to test cosmological models

(D_A, H^{-1}, G_δ, G_Θ, FoG, , New, …)

New physics

Λ

Chameleon type gravity

Probing modified gravity

$d\boldsymbol{\delta}_m/dt + \boldsymbol{\theta}_m/a = 0$

$d\boldsymbol{\theta}_m/dt + H\boldsymbol{\theta}_m = k^2\boldsymbol{\psi}/a$

$k^2\, \boldsymbol{\phi} = 3/2\, H_0^2\Omega_m\, \boldsymbol{\delta}_m/a\, F(\boldsymbol{\epsilon})$

$k^2\, \boldsymbol{\psi} = -3/2\, H_0^2\Omega_m\, \boldsymbol{\delta}_m/a\, G(\boldsymbol{\epsilon})$

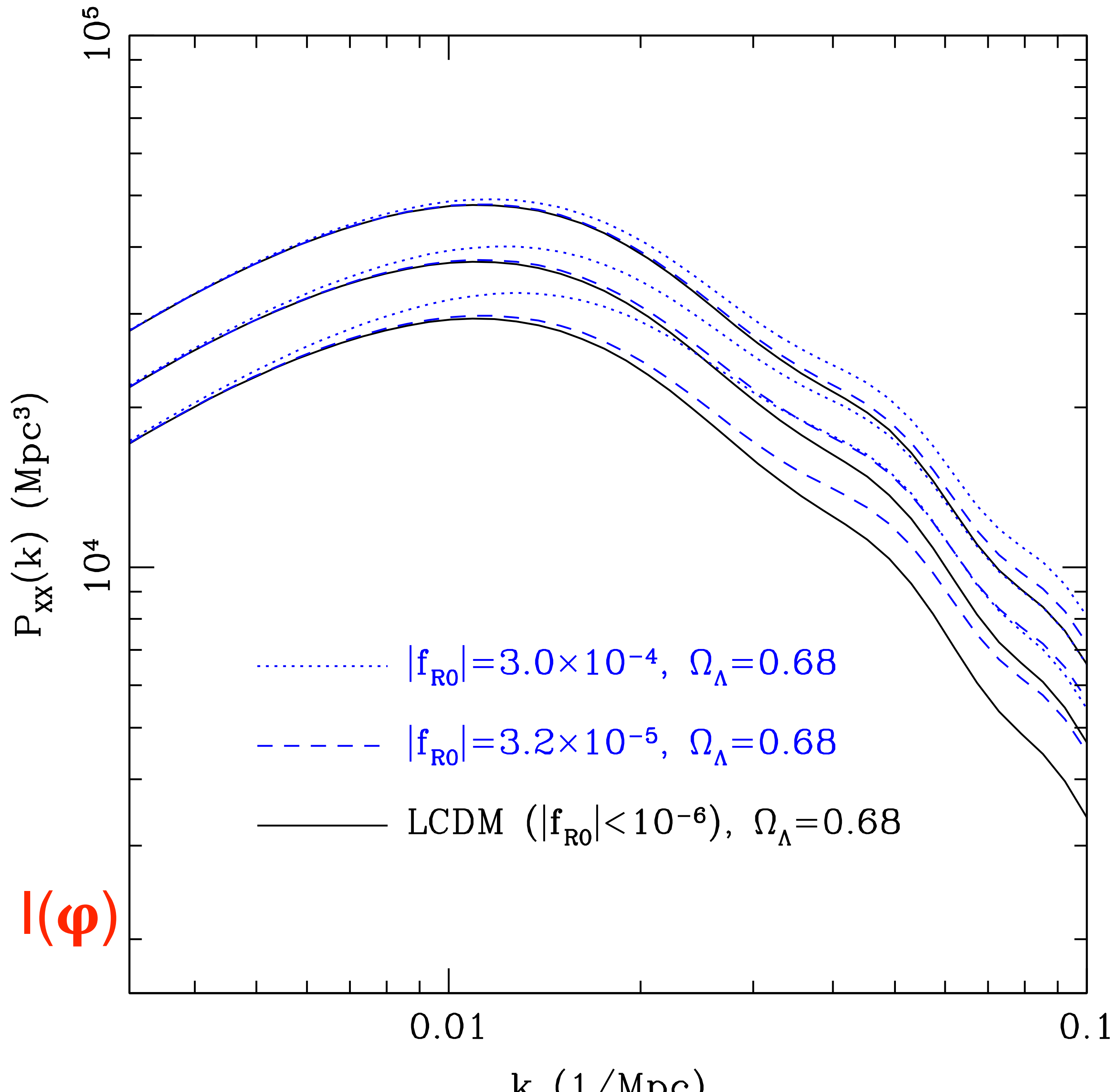

$\boldsymbol{\phi}_{fR} - \boldsymbol{\psi}_{fR} = \boldsymbol{\varphi}$

$k^2\, \boldsymbol{\psi} = -3/2\, H_0^2\Omega_m\, \boldsymbol{\delta}_m/a - 1/2\, k^2\boldsymbol{\varphi}$

$(1+w_{BD})\, k^2/a^2\, \boldsymbol{\varphi} = 3H_0^2\Omega_m\, \boldsymbol{\delta}_m/a - I(\boldsymbol{\varphi})$

$I(\boldsymbol{\varphi}) = M_1(k)\boldsymbol{\varphi}(k) + 1/2\int\cdots\int d^3k_1\cdots d^3k_n\, M_1(k)\cdots M_n(k)\, \boldsymbol{\varphi}(k_1)\cdots\boldsymbol{\varphi}(k_n)$

YSS et.al. 2015

Probing modified gravity

$d\boldsymbol{\delta}_m/dt + \boldsymbol{\theta}_m/a = 0$

$d\boldsymbol{\theta}_m/dt + H\boldsymbol{\theta}_m = k^2\boldsymbol{\psi}/a$

$k^2\,\boldsymbol{\phi} = 3/2\; H_0{}^2\Omega_m\; \boldsymbol{\delta}_m/a\; F(\boldsymbol{\epsilon})$

$k^2\,\boldsymbol{\psi} = -3/2\; H_0{}^2\Omega_m\; \boldsymbol{\delta}_m/a\; G(\boldsymbol{\epsilon})$

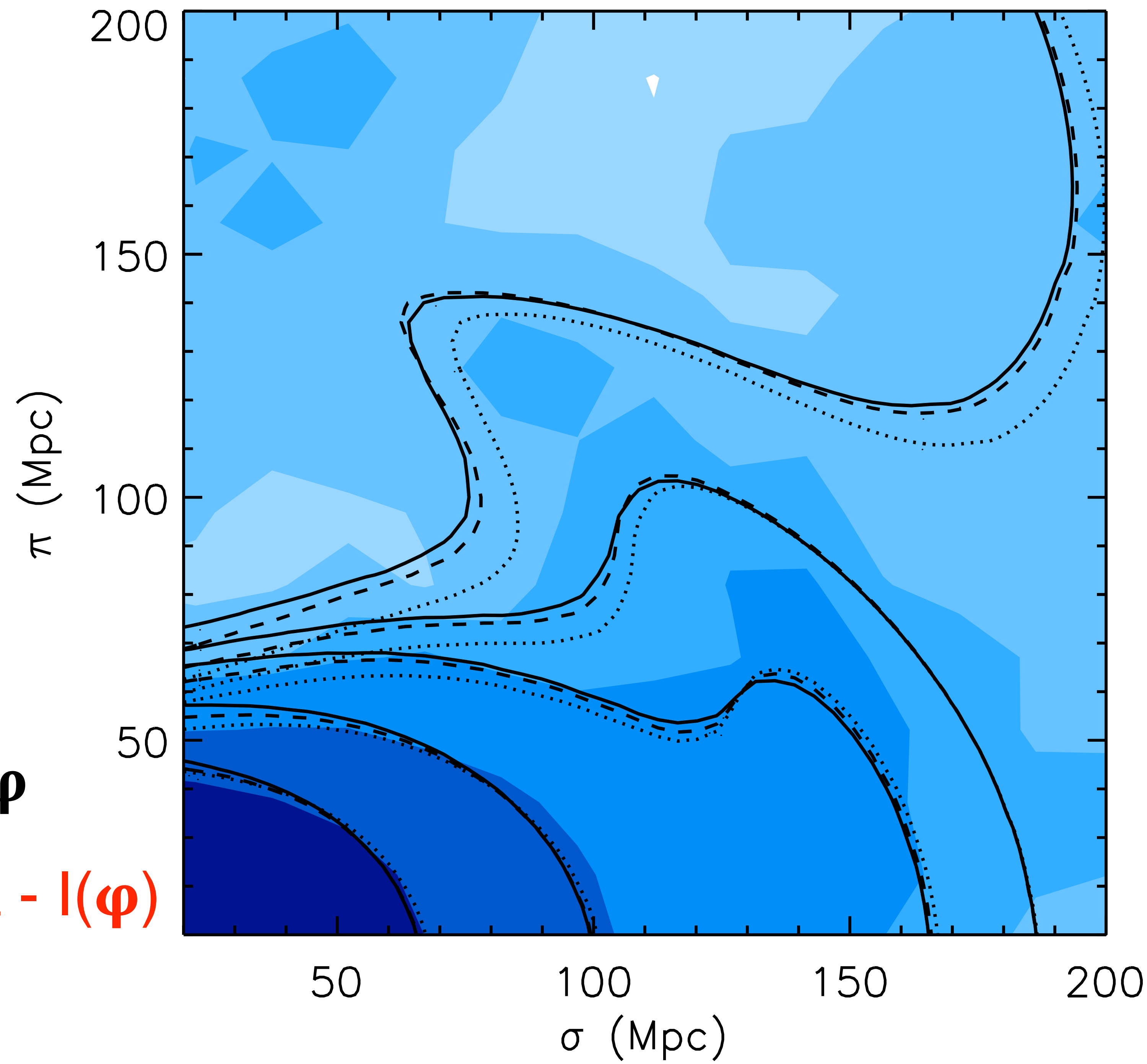

$\boldsymbol{\phi}_{fR} - \boldsymbol{\psi}_{fR} = \boldsymbol{\varphi}$

$k^2\,\boldsymbol{\psi} = -3/2\; H_0{}^2\Omega_m\; \boldsymbol{\delta}_m/a - 1/2\; k^2\boldsymbol{\varphi}$

$(1+w_{BD})\; k^2/a^2\, \boldsymbol{\varphi} = 3H_0{}^2\Omega_m\; \boldsymbol{\delta}_m/a - I(\boldsymbol{\varphi})$

$I(\boldsymbol{\varphi}) = M_1(k)\boldsymbol{\varphi}(k) + 1/2\int\cdots\int d^3k_1\cdots d^3k_n\, M_1(k)\cdots M_n(k)\; \boldsymbol{\varphi}(k_1)\cdots\boldsymbol{\varphi}(k_n)$

YSS et.al. 2015

Probing modified gravity

(D_A, H^{-1}, G_δ, G_Θ, FoG, $|f_{R0}|$)

We find new constraints on f(R) gravity models using BOSS DR11

$|f_{R0}| < 8\times10^{-4}$ at 95% confidence limit

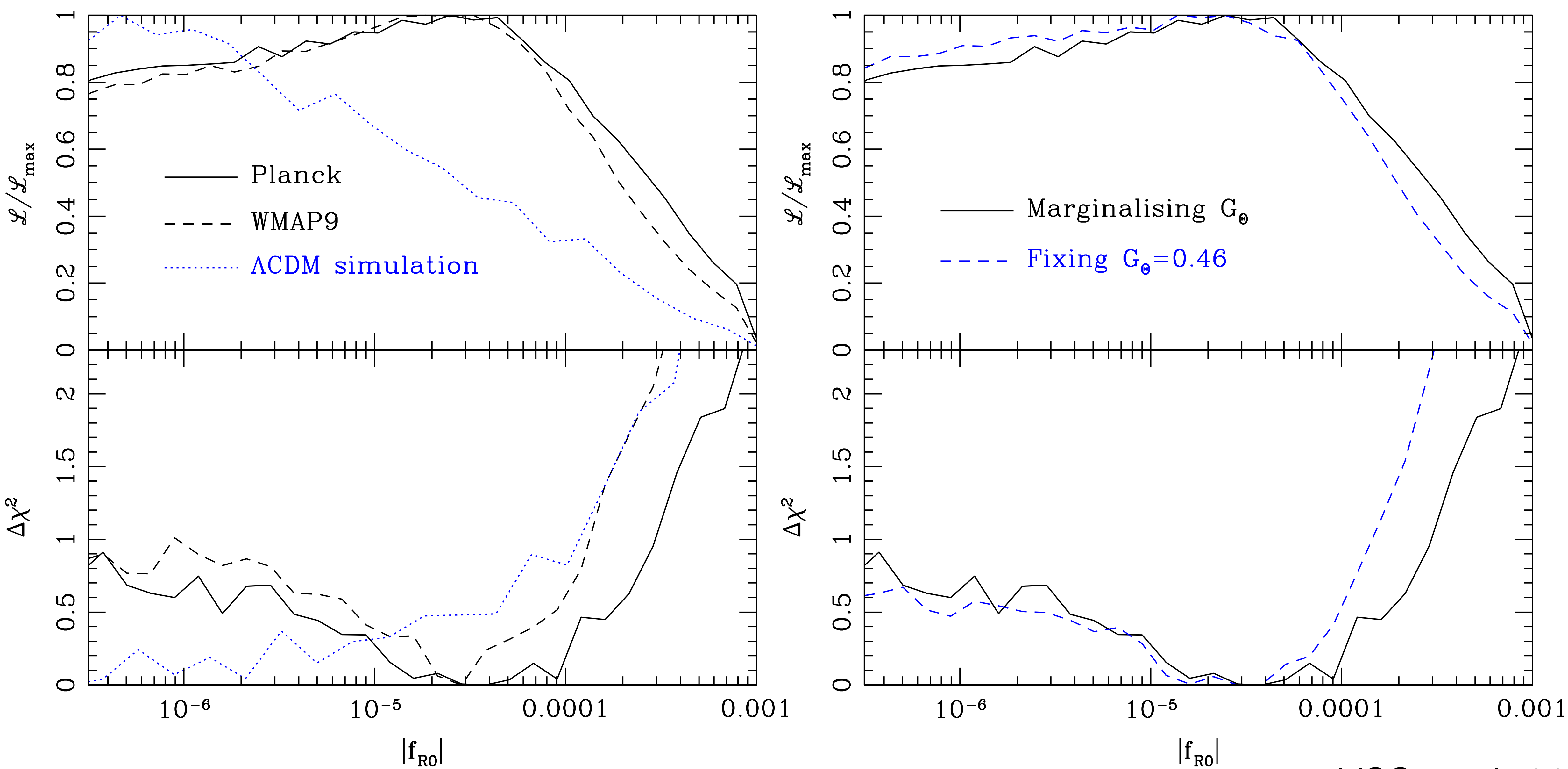

YSS et.al. 2015

Open new window to test cosmological models

(D_A, H^{-1}, G_δ, G_Θ, FoG, New, , …)

Standard model

Massive neutrino

Λ

See Minji's Talk on Fri

Constraints on initial conditions

With the given horizon scale survey, we are accessible to initial condition FoM

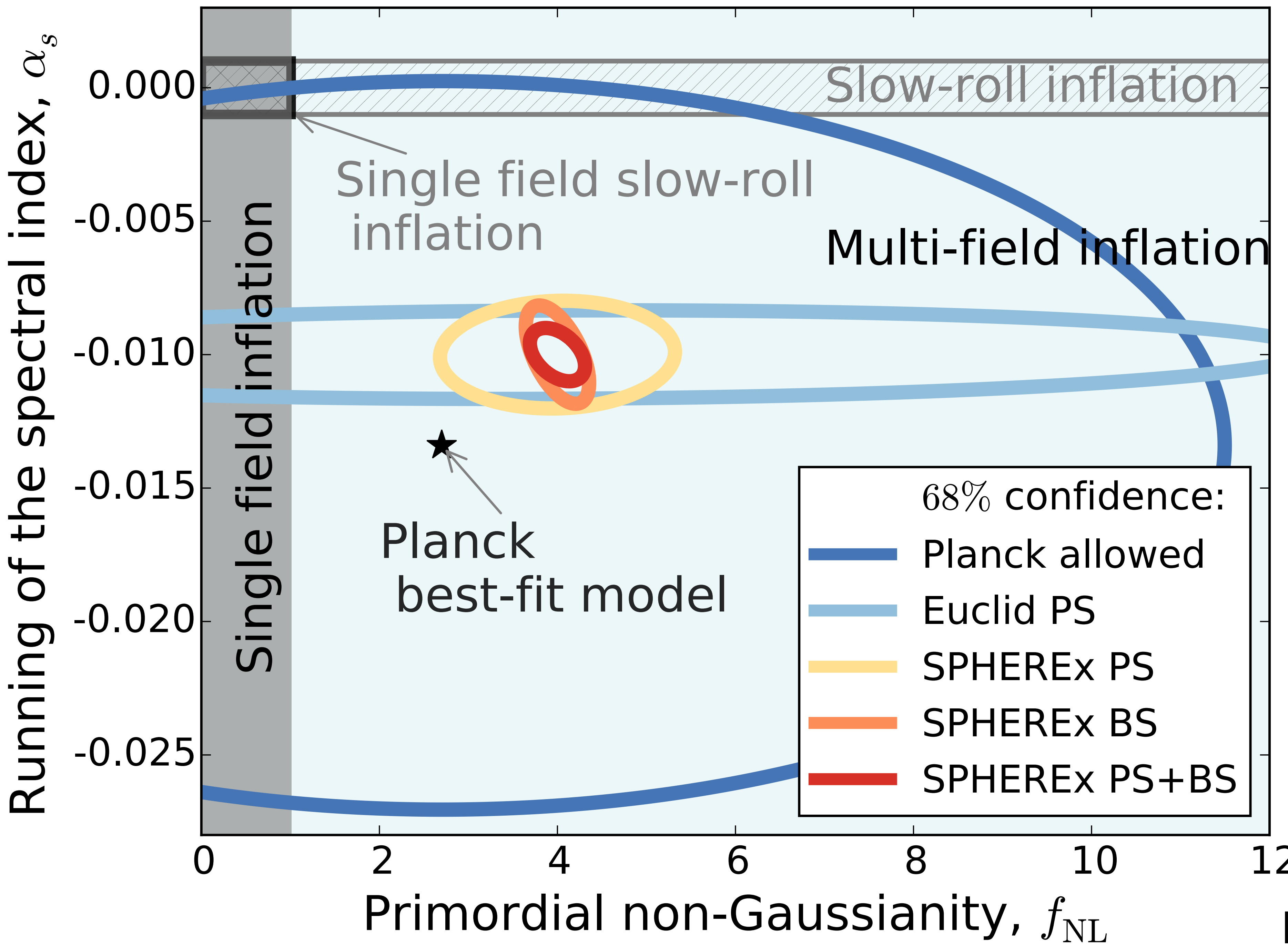

Dore et.al. 2015

Full covariance approach

Fisher matrix is given by

$$F_{\alpha\beta} = \boldsymbol{\Sigma}_k \boldsymbol{\Sigma}_{k1k2k3} \, (\boldsymbol{\partial}S/\boldsymbol{\partial}p_\alpha) \, C^{-1} \, (\boldsymbol{\partial}S/\boldsymbol{\partial}p_\beta)$$

where the vector field S is given by

$$S = \begin{pmatrix} P(k,\mu) \\ B(k_1,k_2,k_3,\mu_1,\mu_2) \end{pmatrix}$$

The full covariance matrix is given by,

$$C^{-1} = \begin{pmatrix} M & -MC_{PB}C_{BB}^{-1} \\ -C_{BB}^{-1}C_{BB}^{-1}M & C_{BB}^{-1}+C_{BB}^{-1}C_{Bp}MC_{PB}C_{BB}^{-1} \end{pmatrix}$$

This full covariance calculation is performed for DESI forecast.

Full covariance approach

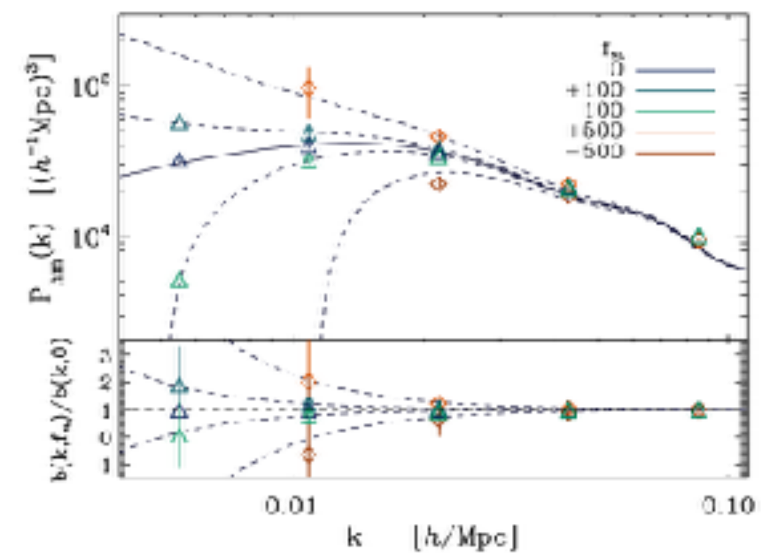

Fisher matrix is given by

$$F_{\alpha\beta} = \Sigma_k \Sigma_{k1k2k3} (\partial S/\partial p_\alpha)\ C^{-1}$$

where the vector field S is given by

$$S = \begin{pmatrix} P(k,\mu) \\ B(k_1,k_2,k_3,\mu_1,\mu_2) \end{pmatrix}$$

The full covariance matrix is given by,

$$C^{-1} = \begin{pmatrix} M & -MC_{PB}C_{BB}^{-1} \\ -C_{BB}^{-1}C_{BB}^{-1}M & C_{BB}^{-1}+C_{BB}^{-1}C_{Bp}MC_{PB}C_{BB}^{-1} \end{pmatrix}$$

This full covariance calculation is performed for DESI forecast.

Bispectrum in redshift space

$B(k_1,k_2,k_3,\boldsymbol{\mu}_1,\boldsymbol{\mu}_2) = D^B{}_{FoG}\, B^{PT}(k_1,k_2,k_3,\boldsymbol{\mu}_1,\boldsymbol{\mu}_2)$

$B^{PT}(k_1,k_2,k_3,\boldsymbol{\mu}_1,\boldsymbol{\mu}_2)$
$= 2[Z_2(k_1,k_2)Z_1(k_1)Z_2(k_2)P(k_1)P(k_2) + \text{cyclic}]$

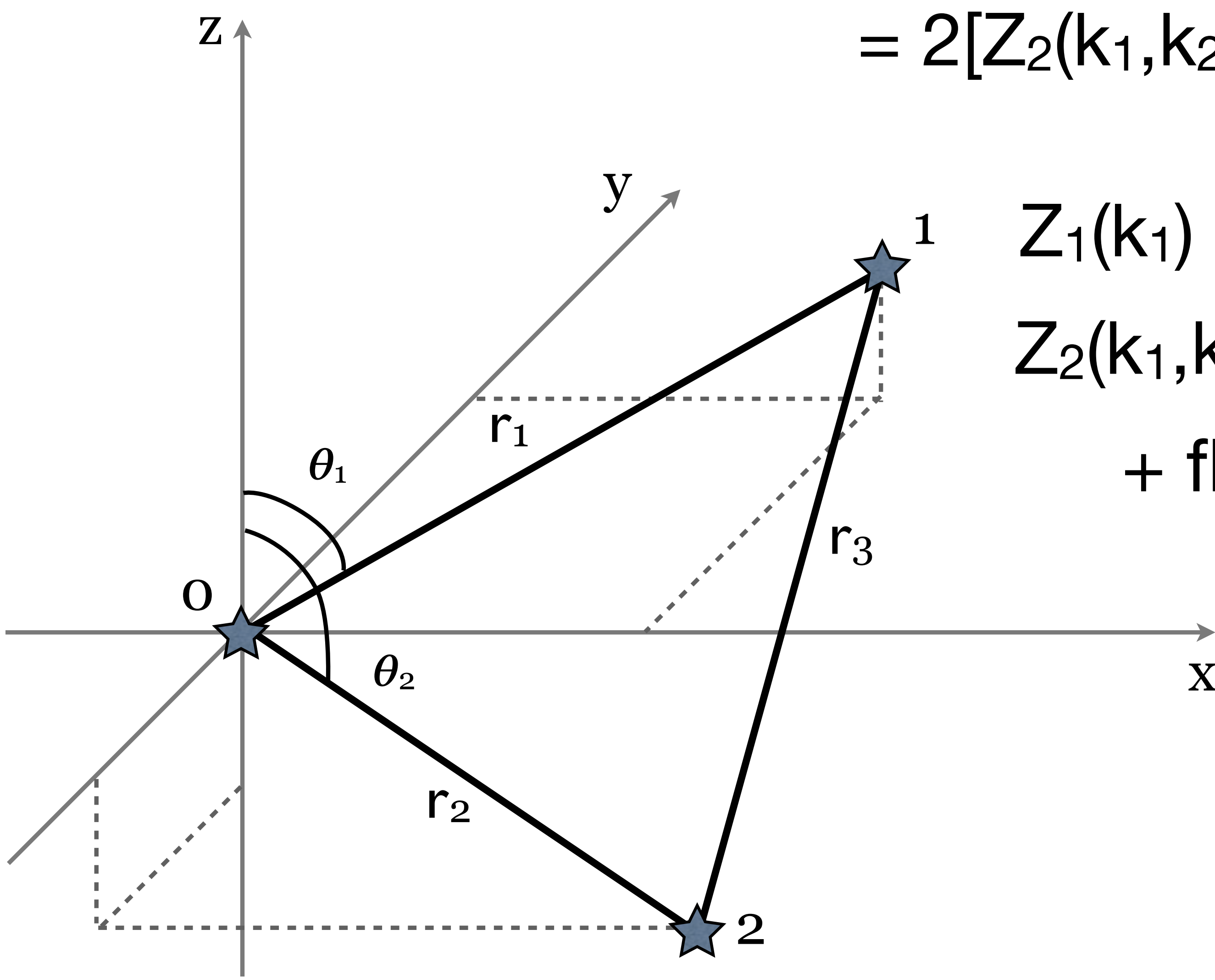

$Z_1(k_1) = b+f\boldsymbol{\mu}_1{}^2$

$Z_2(k_1,k_2) = b_2/2 + bF_2 + f\boldsymbol{\mu}_{12}G_2$
$+ fk_{12}\boldsymbol{\mu}_{12}/2[\boldsymbol{\mu}_1/k_1Z_2(k_2)+\boldsymbol{\mu}_1/k_1Z_2(k_2)]$

Sabiu, YSS 2016 prepared

YSS, Taruya, Akira 2015

Full covariance approach

Fisher matrix is given by

$$F_{\alpha\beta} = \Sigma_k \Sigma_{k1k2k3}\, (\partial S/\partial p_\alpha)\, C^{-1}\, (\partial S/\partial p_\beta)$$

where the vector field S is given by

$$S = \begin{pmatrix} P(k,\mu) \\ B(k_1,k_2,k_3,\mu_1,\mu_2) \end{pmatrix}$$

The full covariance matrix is given by,

$$C^{-1} = \begin{pmatrix} M & \cancel{MC_{PB}C_{BB}^{-1}} \\ -\cancel{C_{BB}^{-1}C_{BB}^{-1}M} & C_{BB}^{-1}+C_{BB}^{-1}C_{Bp}MC_{PB}C_{BB}^{-1} \end{pmatrix}$$

This full covariance calculation is performed for DESI forecast.

The ultimate cosmological test on GR

- Sp
  hav
  obs
  me
  fun
  Wig
- Mo
  will

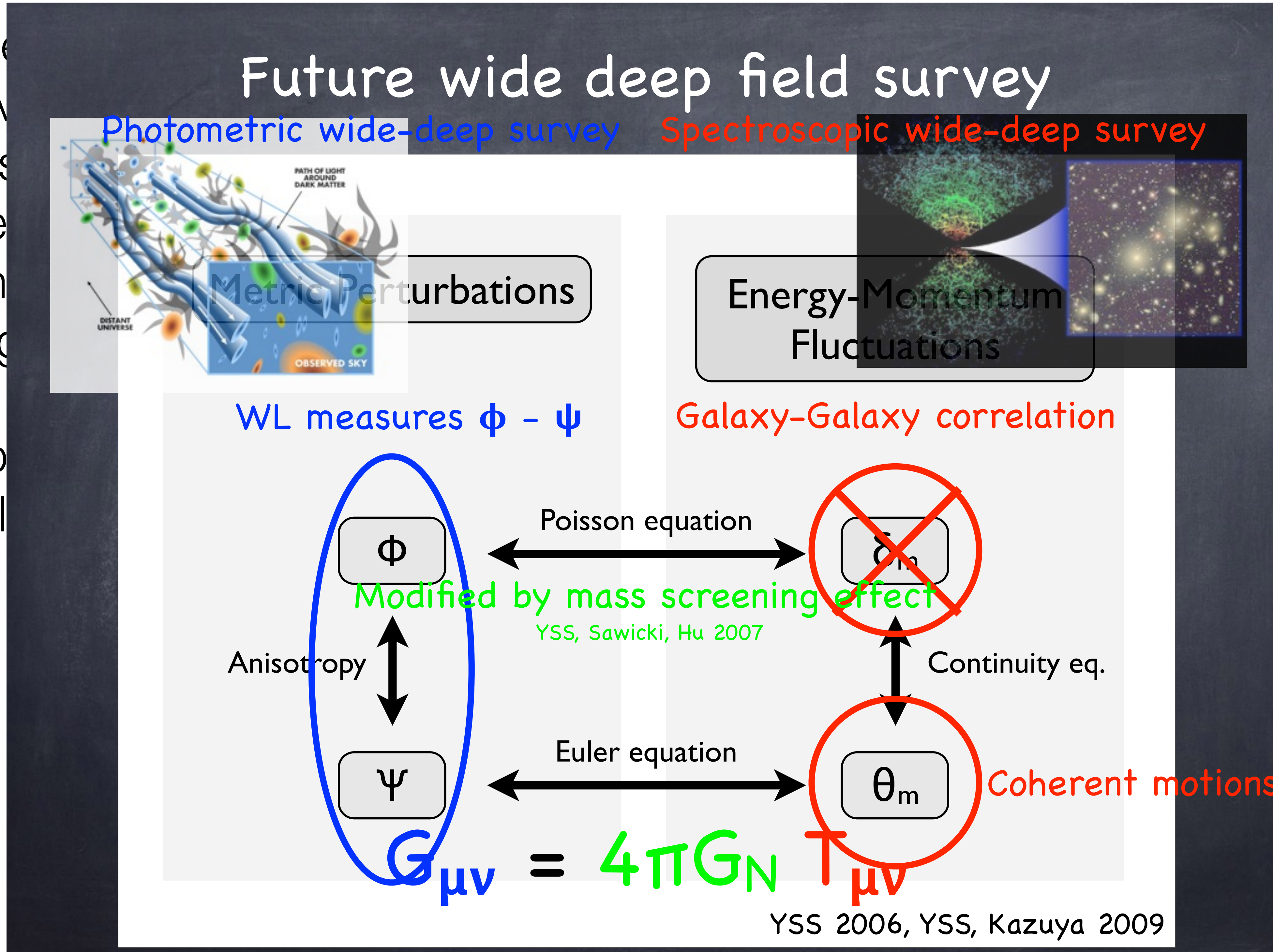

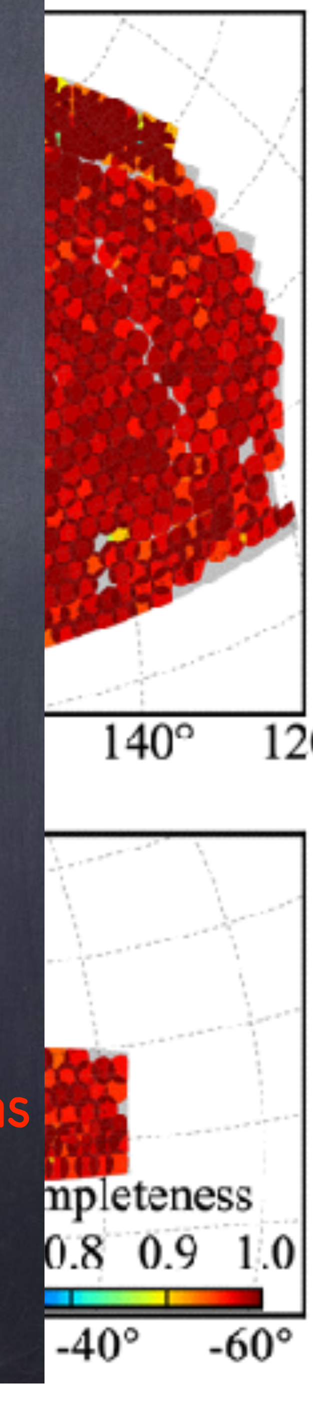

Conclusion

- We are confident of precise and accurate measurements of growth functions within 1% fractional error, for the cosmological model in which growth function evolves coherently.
- The same method can be applicable for modified gravity and massive neutrino constraints, but we need to produce those simulation.
- Spectroscopy survey provides us with a way to test initial conditions using inflationary parameter FoM. It makes sense that we cover as much as sky we can, to access to horizontal scale.
- The southern sky coverage is attractive to the community who is looking for test of GR cosmologically.
- We are nearly ready to maximally exploit the informations provided to us in next decade.